Nylon Refrigerant Tubing

P. H. Geil and F. Rybnikar

ACRC TR-52 October 1993

For additional information:

Air Conditioning and Refrigeration Center
University of Illinois
Mechanical & Industrial Engineering Dept.
1206 West Green Street
Urbana, IL 61801

(217) 333-3115

Prepared as part of ACRC Project 16
Nylon Refrigerant Tubing
P. H. Geil, Principal Investigator

The Air Conditioning and Refrigeration Center was founded in 1988 with a grant from the estate of Richard W. Kritzer, the founder of Peerless of America Inc. A State of Illinois Technology Challenge Grant helped build the laboratory facilities. The ACRC receives continuing support from the Richard W. Kritzer Endowment and the National Science Foundation. The following organizations have also become sponsors of the Center.

Acustar Division of Chrysler
Allied-Signal, Inc.
Amana Refrigeration, Inc.
Carrier Corporation
Caterpillar, Inc.
E. I. du Pont de Nemours & Co.
Electric Power Research Institute
Ford Motor Company
General Electric Company
Harrison Division of GM
ICI Americas, Inc.
Johnson Controls, Inc.
Modine Manufacturing Co.
Peerless of America, Inc.
Environmental Protection Agency
U. S. Army CERL
Whirlpool Corporation

For additional information:

Air Conditioning & Refrigeration Center
Mechanical & Industrial Engineering Dept.
University of Illinois
1206 West Green Street
Urbana IL 61801

217 333 3115

NYLON REFRIGERANT TUBING

Final Report

This project was designed to investigate and characterize the relationship between the structure and properties of nylon tubing materials used in mobile air conditioners, as a function of processing history, temperature and environment. The focus was on the effects of physical aging on structure and properties, and the effect of structure and morphology on coolant (R12 and 134A) diffusion through these materials.

Accomplishments

This research was initiated in October 1990 with funding for 2 years. The project was completed in July 1993, with no additional funding. The most important accomplishments include:

1. Measurements of refrigerant permeation rates at room temperature and 80°C (175°F) through a variety of nylons of current and potential use as tubing materials (summarized in Part A below).

2. Characterization of aging effects at various elevated temperatures, in water and air environment, primarily of four representative nylon tubing materials (described in Part B).

3. Physical characterization of new, potential nylon tubing materials based on nylon 6/66 blends and copolymers (described in two publications; summarized in Part C).

A. Refrigerant Permeation Measurement

Permeation, as used here, describes the weight loss of refrigerant through the sample per unit time (here milligrams/day) and is a function of both the diffusion coefficient (which is a function of the refrigerant concentration gradient through the sample) and the solubility. Permeability coefficients, for the films, will be given in units mg/day - in^2 - 0.001", i.e. corrected for cross-sectional area and thickness of the film.

1. Experimental method and leakage rate measurements.

The initial goal of the project involved measuring permeation in nylon tubes prepared under various processing methods at Parker Hannifin. Their methods for measuring permeation involved changes in weight of actual coated, overbraided tubes sealed with mechanical joints at the ends. This method turned out not to be feasible, both because the tubes without the overbraiding were not strong enough to support the required pressures and because of Parker-Hannifin's withdrawal from the Center preventing the fabrication of tubes. Thus a cup method using compression molded sheets was adapted; this permits variation in thermal history and composition but not orientation. O-rings were used for seals; as described below this was a major problem. The cup method, as compared to other possible methods (quartz balance, gas chromatography or pressure drop) has the advantage of simplicity, high sensitivity and ease of running numerous samples simultaneously. With duplicate measurements being made on some 20 materials, these advantages were of particular concern.

The cup assembly design is shown in Fig. 1. They are made from aluminum and consist of a threaded cup with a groove for an O-ring and 2 holes in the bottom enabling tightening by a large jig. For measurements the refrigerant is first liquefied by passing through a Cu-coil cooled to -80°C in

methanol. The liquid coolant (10-30g) is poured into the precooled cup; the cup is covered by the polymer sheet to be measured, topped by a bronze or steel mesh sheet and a perforated aluminum plate. The mesh is of the same diameter as the film, the mesh permitting escape of the gas after diffusion through the film; both film and mesh extend beyond the O-ring. The assembly is tightly sealed against the 2.25 inch diameter O-ring. The initial O-ring groove depth (0.078") is that recommended for a 0.10" thickness ring. After the temperature equilibrates the weight loss of refrigerant is measured using an analytical balance with a sensitivity of 0.0001 gm. Measurement are done at room temperature every 1 or 2 days with the cups being held either at room temperature or in an oven. After attaining room temperature in the cup, coolant liquid and vapor coexists, the saturated vapor pressure depending on temperature. The saturated vapor pressure of R12 at room temperature is 85 psi.

The crucial problem for most diffusion methods is to eliminate possible leakage or losses of diffusant by other ways than diffusion through the sample sheet. This is of particular importance in our case because we are dealing with materials that are supposed to have a very high diffusion resistance for refrigerants. Preliminary leakage tests were done with two O-rings recommended for fluorocarbons. Neoprene 70 and Buna N Table I lists the characteristics of various O-ring compounds relative to refrigerant sealing. Buna O-rings showed a better sealing property in blank experiment runs using a solid Al plate instead of the polymer sheet. The weight loss in these blank experiments, run for 11 days, was in the range 0 - 0.2 mg

Typical weight loss curves of blank samples (no nylon or screen, solid aluminum top) for 25 days are shown in Figs. 2 and 3 for Buna N (Nitrile in table) and Neoprene with the original groove depth. Despite Neoprene having a ranking of 1 as compared to 2 for Buna N, it lost more than 3 times as much

refrigerant per day as Buna N (13 mg/day versus 4 mg/day) at room temperature (ca. 22°C) after an ca. 8 day induction period. Furthermore, it is clear from Fig. 2 that permeation at 80°C (175°F) is much higher than at 22°C. The 80°C samples were placed in an oven between the room temperature weighing.

The fact that the cups for the above had to be screwed down very tightly to prevent leaks suggested there was insufficient play to fully compress the O-ring. In addition, clearly permeation through the O-ring was occurring. It is noted initial blank tests were run for only 11 days. Due to the induction time, corresponding to the time required to diffuse through the O-ring and set up the concentration gradient, Buna N looked like an excellent candidate; after the induction period however, it clearly had too high a permeation rate.

Remachining the cups to a 0.066" groove depth, permitting greater compression (and therefore a longer permeation path), reduced the permeation rate to 2 mg/days (Fig. 4) for the Buna N and increased the induction period to ca. 17 days. Simultaneously Viton O-rings were obtained (fluorocarbon, also with a 1 rating, including in the presence of oil) and tested; the results are shown in Fig. 5 for both the 0.076 and 0.066 depth groove. Although the induction periods are similar the improvement in permeation rate with decreased groove depth is striking. Following the induction period the ratio is ca. 2.5 mg/day.

Increasing the compression, on both Viton and Buna N, by using a 0.060" groove, further improved the leak rate (Fig. 6). Viton is again seen to be better than Buna N, with the variations in leakage rate being attributed to variations in the degree of compression and leakage through the O-ring -metal seal. The compression was sufficient that flow of the aluminum apparently occurs, the cups becoming extremely difficult to unscrew after being sealed for several days. Up to 40 days no clear induction period is seen for the Viton; for the Buna N it

would appear to be ca. 22 days. Leakage rates for the Viton are on the order of 0.13 mg/day at room temperature. At 80° (Fig. 7) leakage rates are higher (1 mg/day) for Viton, as would be expected from the higher vapor pressures, higher solubility and increased polymer molecular mobility. All 80° samples were run with the same sealed cups as for (and after) the room temperature runs. The lack of an induction period suggests rapid development of the new equilibrium concentration gradient, assuming one was completed at room temperature.

Using the 0.060" groove blanks were run with refrigerant 134a (Fig. 8). The leakage rate increases in the order Neoprene-Viton-Buna N. Viton was chosen, however, for use with the nylon films because of potential problems with lubricating oils. For Viton the leakage rate is 0.2 mg/day after an induction period of about 22 days. At 80°C, the leakage rates are also higher with 134a, the O-ring materials remaining in the same order (Fig. 9). For Viton it is ca. 2.3 mg/day, similar to that for R12. Again no induction period is seen, the same filled cups being used for the room temperature and, subsequently, 80°C measurements.

2. Materials.

Refrigerants R 12 (Racon, Inc.) and 134a (Forane, Elf Atochem North America, Inc.) were used as supplied in 30 lb. cylinders. For filling the cups it was cooled to -80°C, the cups being previously cooled in liquid nitrogen. The cups were sealed while cold.

Initial polymer nylon tubing material was supplied by Parker Hannifin. All of these materials, as described in Table II, are modified with added polyolefin copolymer and/or a plasticizer, as well as two of them being copolymers of nylon 6 and 66. The copolymers would be expected to have lower

crystallinity (lower stiffness, higher diffusion rate) than the homopolymers. The polyolefin is added for toughness, the plasticizer for flexibility.

Subsequently a wide variety of "pure" nylon copolymers and blends were obtained from DuPont (prepared and/or supplied by Dr. A. Elia). The copolymers were commercial Zytel (DuPont) samples; their composition is shown in Table III. Selected resins from these materials were used for the diffusion studies and for the aging and interface studies described in Parts B-C.

The films were made by compression molding, with a nominal thickness of 0.010". Film thicknesses were measured for calculation of the permeability.

3. Nylon film permeability measurements.

Representative curves for 2 samples, Selar OH* and nylon 6 (PA6) are shown in Fig. 10. The samples were run simultaneously using the 0.060" groove cups; the coincidental variations in weight are attributed to changes in moisture absorption due to changes in relative humidity. They are not seen for the blank runs. There is no obvious induction time, the PA6 samples possibly having a 20 day induction time. Duplicates were run for all of the samples, the variation between runs being similar to that shown or worse (see below). Weight loss/day measurements were taken by assuming no induction period, drawing a straight line through all of the data. Permeation coefficients were calculated after subtracting the O-ring permeation rate. Values are shown in Table IV. It is noted that during the induction period, for O-ring and/or nylon film, there should be essentially no weight loss; it is during this time that the diffusion front is moving through the barrier and an equilibrium concentration gradient is being set up. All leakage during this time is presumably due to problems in the O-ring-metal

---

* Described by DuPont as a "barrier resin".

and O-ring-nylon seal. Thus leakage rate and permeation rates listed are all maximum values, actual rates being lower.

As indicated by the duplicate values listed for Zytel 91 AHS and PA6 reproducibility was not too good; that for PA6 was the best. In many cases one of the duplicate cells would have a low leakage rate for an extended period and then suddenly begin to leak at a high but uniform rate. For instance, for the Selar OH sample shown, the second cell had the same leakage rate as that shown in Fig. 10 for 20 days and then began to leak at a rate of 1.9 mg/day. The transition time varied from a few days to more than 20. Since it was never seen for a blank (O-ring only) samples, it is attributed to a failure of the nylon. It is possible that either a thin region in the film gave under the pressure (e.g. one side of a bubble; it clearly is not a pinhole) or some portion of the nylon at the edge underwent deformation due to the high clamping pressure. The initial wt. loss/day for nearly all of the samples showing a transition was essentially the same as that listed, i.e. similar to the relative values for PA6. The Zytel 91AHS samples on the other hand, showed no transition, remaining linear with a high weight loss rate over the entire test period.

Clearly, based on the scatter in the experimental data and the similarity in leakage rates of the film and the O-ring, it is not possible to rank the various nylons tested; indeed 3 of the samples had a lower weight loss/day than the assumed O-ring leakage rate. The high value for Zytel 91 AHS we believe is correct and likely related to the high amount of plasticizer in the sample (Table II); permeation through the plasticizer rich (amorphous) regions is expected to be rapid. Just as clear, however, is the observation that O-ring seals should not be used for R12 or 134a. When compressed in the 0.060" groove the diffusion path will be on the order of 0.1" or larger (as indicated by the compression mark on

the films) and the area of the O-ring exposed to the refrigerant is much less than for the film.

At 80°C, as would be expected due to the higher vapor pressure of the R12, weight loss rates are much higher. The values listed are for the same films and cells as run at 22°C; after the 22°C run the cells were place in an 80°C oven. The scatter is even larger, but with nearly all values being considerably higher than the 1 mg/day attributed to the O-rings. For both environmental and economic regions it would appear nylons are not to be recommended for extended use with R12 at 80°C (i.e. 175°F).

The data for a number of nylon samples (single runs only, not shown are those developing rapid leaks) with refrigerant 134a at room temperature are shown in Fig. 11. Considering that the O-rings alone would be expected to leak at a rate of 0.2 mg/day (i.e. 18 mg in the 40 days), the permeation rates of all of the nylons would appear excellent. Again, the common variations in weight are attributed to relative humidity effects, these samples being run during the summer (the R12 room temperature samples were run in the winter). The absence of an induction period is in agreement with the conclusion of extremely low permeation rates; the refrigerant apparently not yet reaching the surface of the film or O-ring within the 40 day experimental time. If so, the variations in weight loss rate observed should be entirely attributed to leakage through the contact seals.

At 80°C, a high rate of permeation is again seen, Fig. 12, much larger than the O-ring leakage. The weight loss/day for the 2 samples shown was 45 mg/day for PA66 and 70 mg/day for PA6. Despite the much higher vapor pressure, we believe this rate should be attributed to permeation through the nylon, not contact seal leakage.

4. Conclusions.

Despite the scatter in the data, any nylon (homopolymer, copolymer or blend) would appear to be usable for 134a refrigerant tubing at room temperature with permeation rates being lower than for R12. Indeed, diffusion may be so low that we did not observe permeation through the film in the experimental times used. At elevated temperatures (i.e. 80°C), however, permeation becomes of environmental and economic concern, for both R12 and 134a. All O-rings tested, Neoprene, Buna N and Viton are not suitable for seals, even in the absence of lubricating oils, particularly at elevated temperature unless compressed to a much higher degree than normal.

POLYMER KEY Code	Polymer	BASIC PARKER O-RING COMPOUNDS	① TEMPERATURE RANGE °F	°C
A	Polyacrylate	A607-70	0 to + 250/300	- 17 to + 177
B	Butyl	B612-70	- 75 to + 250/300	- 59 to + 120/150
C	Neoprene (Chloroprene)	C873-70	- 45 to + 300	- 43 to + 149
E	Ethylene Propylene	E540-80	- 70 to + 250/400	- 57 to + 100/205
G	SBR	G244-70	- 70 to + 225	- 57 to + 107
L	Fluorosilicone	L677-70	- 100 to + 350/400	- 73 to + 177/205
N	Nitrile (BUNA N)	N674-70	- 30 to + 250	- 34 to + 121
		N103-70	- 65 to + 225	- 55 to + 107
P	Polyurethane	P642-80	- 30 to + 180/225	- 35 to + 82/107
S	Silicone	S604-70	- 65 to + 450	- 54 to + 232
T	Polysulfide	T341-65	- 75 to + 225	- 60 to + 107
V	Fluorocarbon	V747-75	- 15 to + 400/500	- 26 to + 205/260

① These temperature ranges will apply to the majority of fluids for which the compound is recommended, but in some fluids the range may be different. See Figure A3-5.

COMPATIBILITY RATING

1. Satisfactory
2. Fair (Usually OK for static seal)
3. Doubtful (Sometimes OK for static seal)
4. Unsatisfactory
X. Insufficient Data

	RECOMMENDED O-RING COMPOUND NUMBER	DYNAMIC & STATIC								STATIC ONLY			
		Nitrile	Ethyl.-Prop.	Fluorocarb.	Neoprene	SBR	Polyacrylate	Polyureth.	Butyl	Butadiene	Isoprene	Nat. Rubber	Hypalon	Fluorosilic.	Silicone	Polysulfide
		N	E	V	C	G	A	P	B	D	I	R	H	L	S	T
Freon, 11	A607-70	2	4	2	4	4	1	X	4	X	X	4	1	2	4	1
12	C873-70	2	3	1	1	1	X	1	3	4	4	2	1	3	4	1
12 and ASTM Oil #2 (50/50 Mixture)	V747-75	2	4	1	3	4	X	X	4	4	4	4	2	2	4	X
12 and Suniso 4G (50/50 Mixture)	V747-75	2	4	1	3	4	X	X	4	4	4	4	2	2	4	X
Freon, 13	C873-70	1	1	1	1	1	X	X	1	X	1	1	1	4	4	1
13B1	C873-70	1	1	1	1	1	X	X	1	X	X	1	1	2	4	1
14	C873-70	1	1	1	1	1	X	1	1	X	X	1	1	X	4	1
21	•	4	4	4	3	4	X	X	4	4	4	4	4	X	4	4
22	C873-70	4	3	4	1	1	2	4	3	X	X	1	1	4	4	4
Freon, 22 and ASTM Oil #2 (50/50 Mixture)	C873-70	4	4	2	2	4	2	X	4	X	X	4	X	2	4	2
31	C873-70	4	1	4	1	2	X	X	1	X	X	2	2	X	X	3
32	C873-70	1	1	4	1	1	X	X	1	X	X	1	1	X	X	1
112	V747-75	2	4	1	2	4	X	X	4	X	X	4	2	X	4	1
Freon, 113	C873-70	1	4	2	1	2	X	1	4	X	X	4	1	X	4	1
114	C873-70	1	1	1	1	1	X	X	1	X	X	1	X	X	4	1
*Recommend Parker Metal-V-Seal																
Freon, 114B2	C873-70	2	4	2	2	4	X	X	4	X	X	4	1	X	4	2
115,116	C873-70	1	1	2	1	1	X	X	1	X	X	1	X	X	X	1
502	C873-70	2	1	2	1	1	X	X	1	X	X	1	X	X	X	X
Freon, BF	V747-75	2	4	1	2	4	X	X	4	X	X	4	2	X	4	1
C318	C873-70	1	1	2	1	1	X	X	1	X	X	1	1	X	X	1
K-152a	C873-70	1	1	4	1	1	X	X	1	X	X	1	4	X	X	1
K-142b	C873-70	1	1	4	1	1	X	X	1	X	X	2	1	X	X	1
MF	T341-65	2	4	2	4	4	X	3	4	X	X	4	1	X	4	1
PCA	N674-70	1	4	2	1	2	X	1	4	X	X	4	1	X	4	1
TF	N674-70	1	4	2	1	2	X	1	4	X	X	4	1	X	4	1

A1 Suitability of use of various types of O-rings; from Parker Seal Co.

Sample	Co	PA matrix	Ratio	Rubber	%	Additives, b	%
Zytel 91AHS	DuPont	PA6/PA66	15/85	0	0	n-butylsulfonamide	18
Zytel 726	DuPont	PA6		PO-copolymer,a	30-50	?	
8350	Allied	PA6		PO-copolymer,a	28	?	
8358	Allied	PA6/PA66	85/15	PO-copolymer,a	37	n-butylsulfonamide	5

a - probably Surlyn

b - additional 1% of various antioxidants, stabilizers expected.

AII. Nylon tubing materials. These materials (and their composition) were supplied as tubes and resin by Parker Hannifin Co.

Make	Ratio PA-6/66
1. 109 L NCO10 NB 31 E 82	10/90
2. FE 3511 NCO10 NI 1 OE 76	15/85 (+ additive)
3. FE 3511 NCO10 UL13N22	35/65
4. FE 3565 Lot # NA 12 U 19	15/85
5. FE 2400 NCO10 TG 19 A 79	22.5/77.5
6. FE 2370 NCO10 Lot# UK 085L95	10/90
7. 91 AHS NCO10 NF 35 I 55	22.5/77.5 (+ plasticizer)

AIII. Composition of various Zytel 6/66 copolymers, as supplied by Dr. Elia of the DuPont Co.

Material	Type	Sheet Thickness 0.001" inch	Slope a) mg/day /3.9 inch^2 at 22°C	at 80°C	Permeation (0.001" thick) at 22°	Coefficient mg/day/in.^{2} at 80°C
8350	Blend	10.5	.205	2.91	.210	5.61
8358	Blend	10.	.205	32.60	.200	79.00
Z.91 AHS	Blend	10.7	.762	4.67	1.704	9.81
Z.91 AHS	Blend	11.2	.530	8.66	1.134	21.45
PA66	Homopolymer	8.5	.173	9.88	.102	18.87
PA6	Homopolymer	11.1	.200	11.61	.208	29.44
PA6	Homopolymer	10.0	.215	30.10	.225	72.75
PA6/66 1/1	Polymer Blend	7.5	.08	12.10	--	20.81
PA6/66 7/3	Polymer Blend	7.5	.07	14.45	--	25.22
PA/66 1/9	Polymer Blend	8.0	.265	8.18	.280	14.36
Z.109 10/90	Copolymer PA6/66	8.4	.175	5.41	.105	9.26
Z.2400 23/77	Copolymer PA6/66	9.5	.170	9.58	.106	20.38
Z.3511 35/65	Copolymer PA6/66	12.3	.118	7.23	--	19.16
Selar OH		16.0	.163	38.42	.152	149.68

a) Weight loss/day, not corrected for O-ring leakage.

b) Corrected for O-ring permeation, 0.125 and 1 mg/day, but; not corrected for seal leakage as observed during the induction period.

AIV. Weight loss/day and permeation coefficient for various nylon films with R12, at room temperature and 80°C.

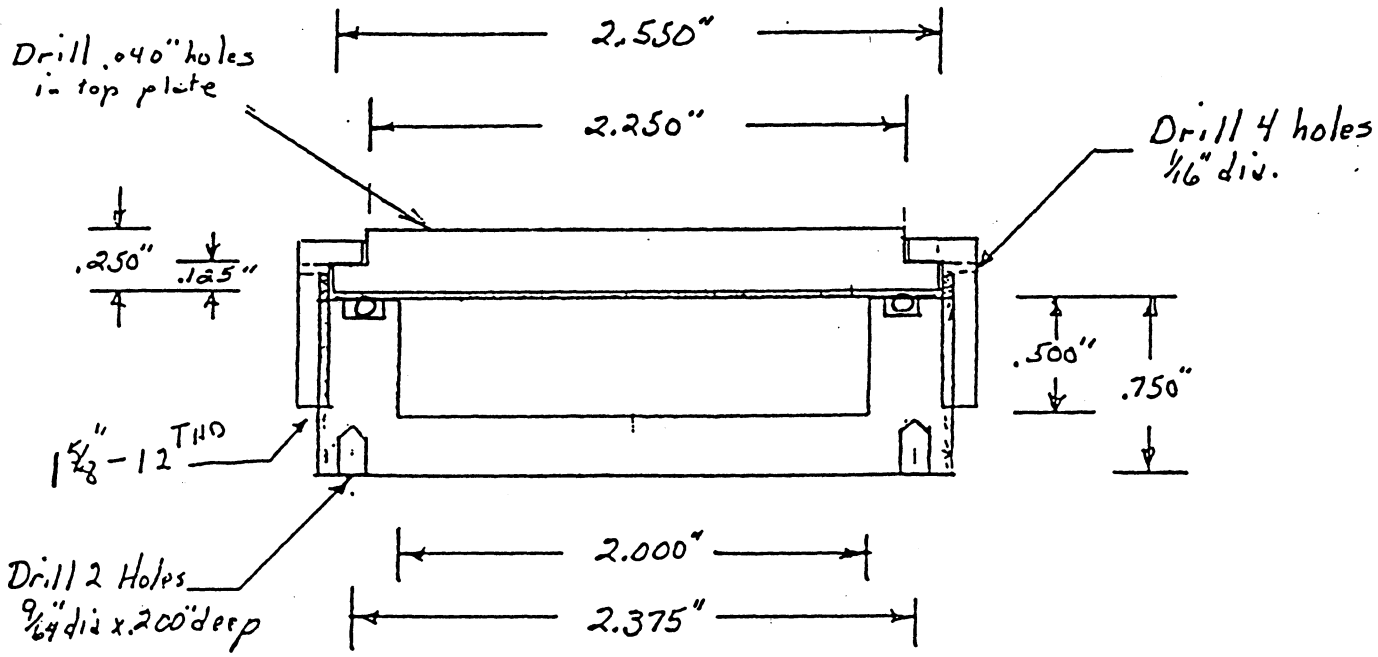

A1. Diagram of the cup assembly. The O-ring groove was initially 0.078" deep and later remachined to first 0.066" and then 0.060" depth. All data shown are for the latter depth unless indicated. A jig was required to screw and unscrew the assembly, maximum possible torque (9" handle) being exerted during tightening.

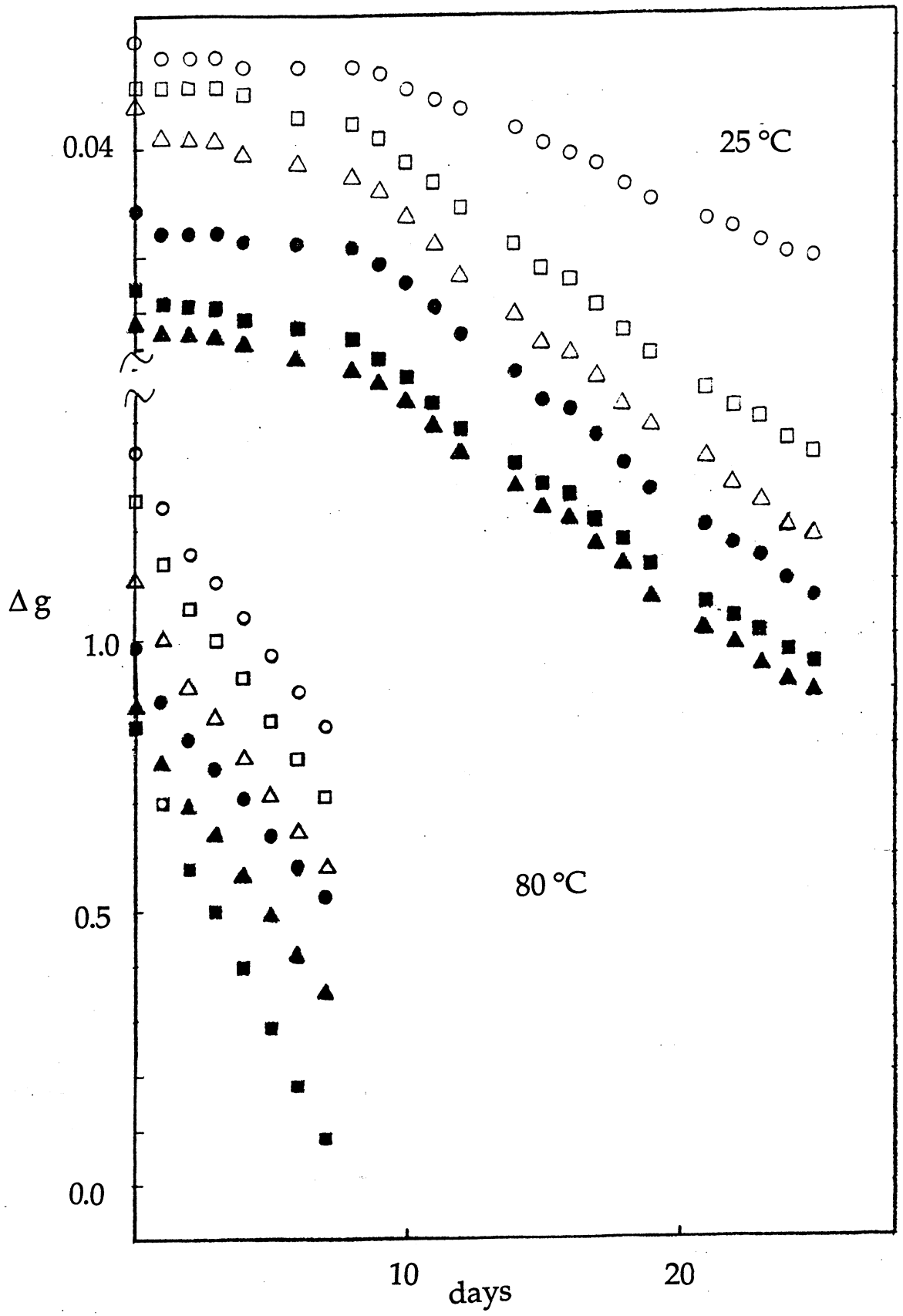

A2. R12 permeation (weight loss) through Buna N O-rings at room temperature and 80°C using the 0.078" deep groove. Induction time ca. 8 day.s

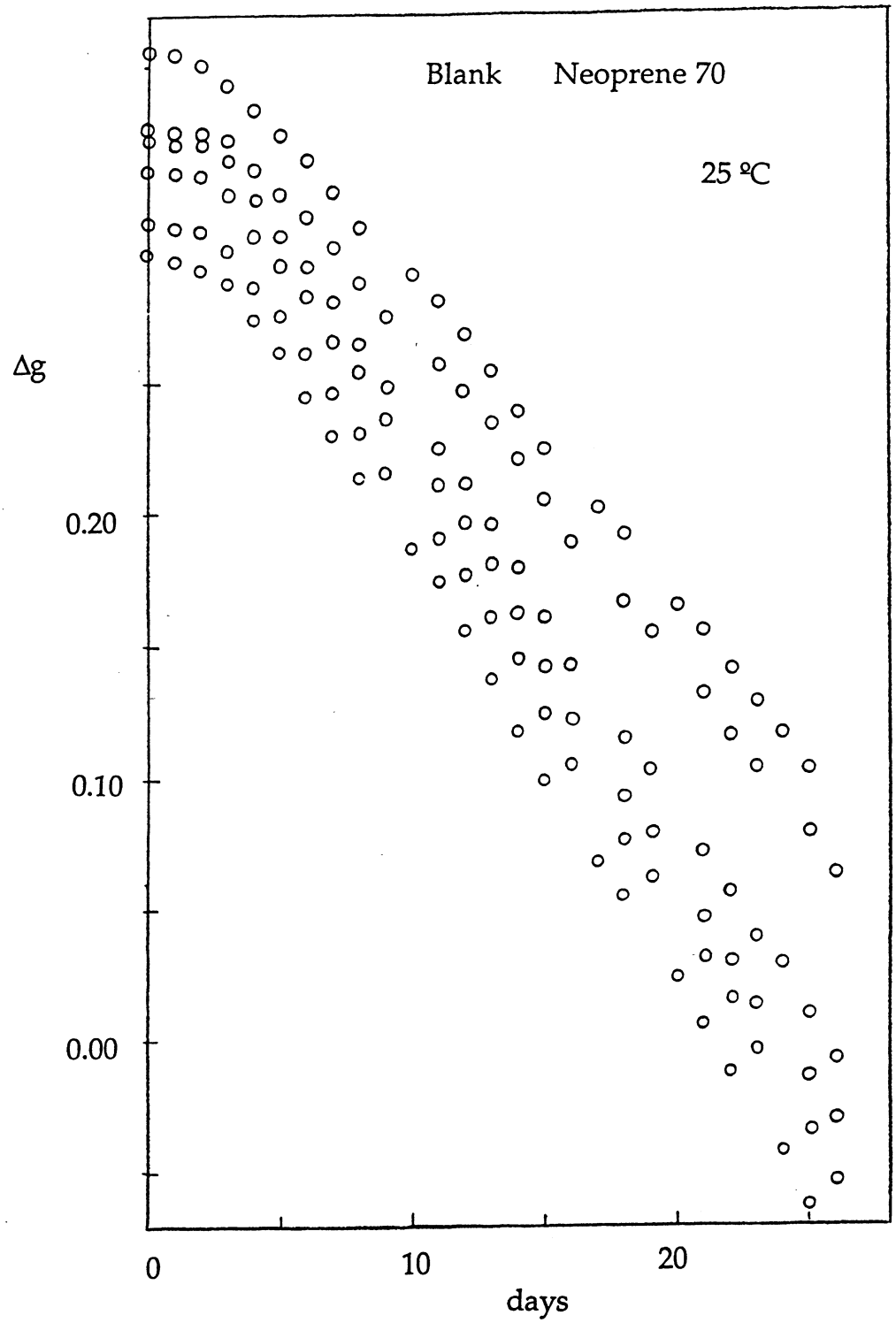

A3. R12 permeation through Neoprene O-rings (0.078" groove) at room temperature. Induction time ca. 2 days.

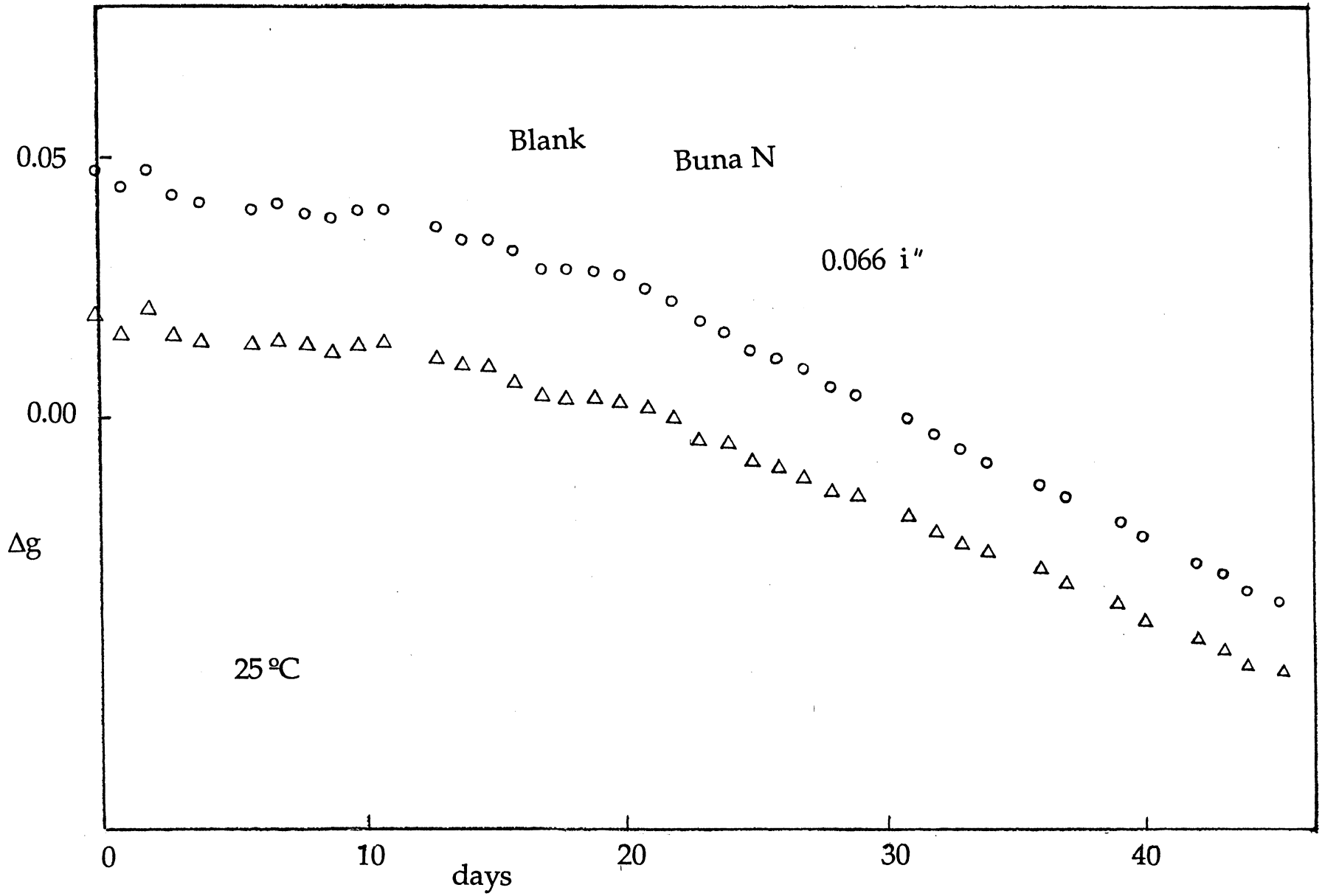

A4. R12 permeation through Buna N O-rings at room temperature (0.066" groove). Induction time ca. 20 days.

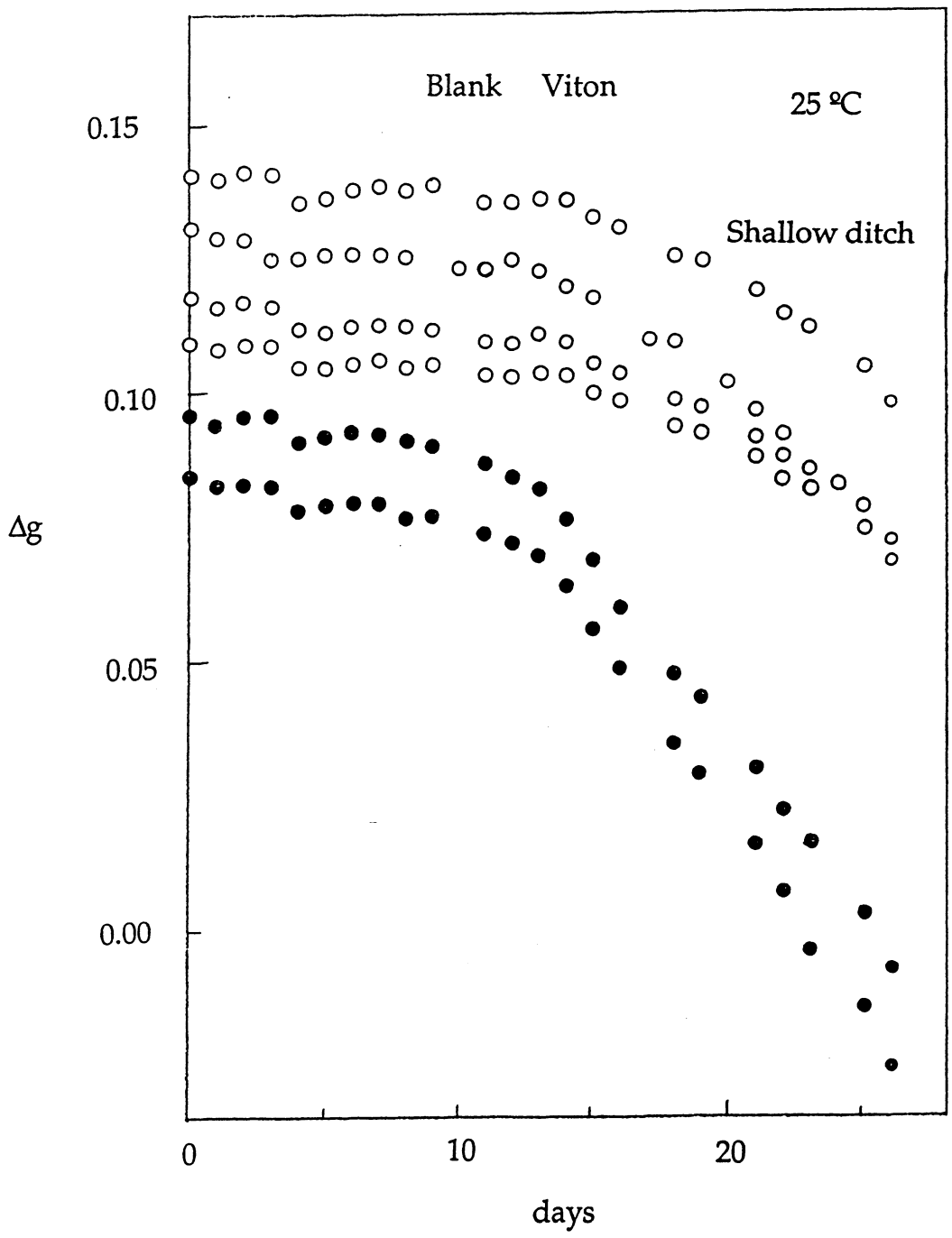

A5. R12 permeation through Viton O-rings at room temperature 0.066" groove (open circles) and 0.078" groove (filled circles). The induction time is longer and the "leakage" rate lower with the shallower groove.

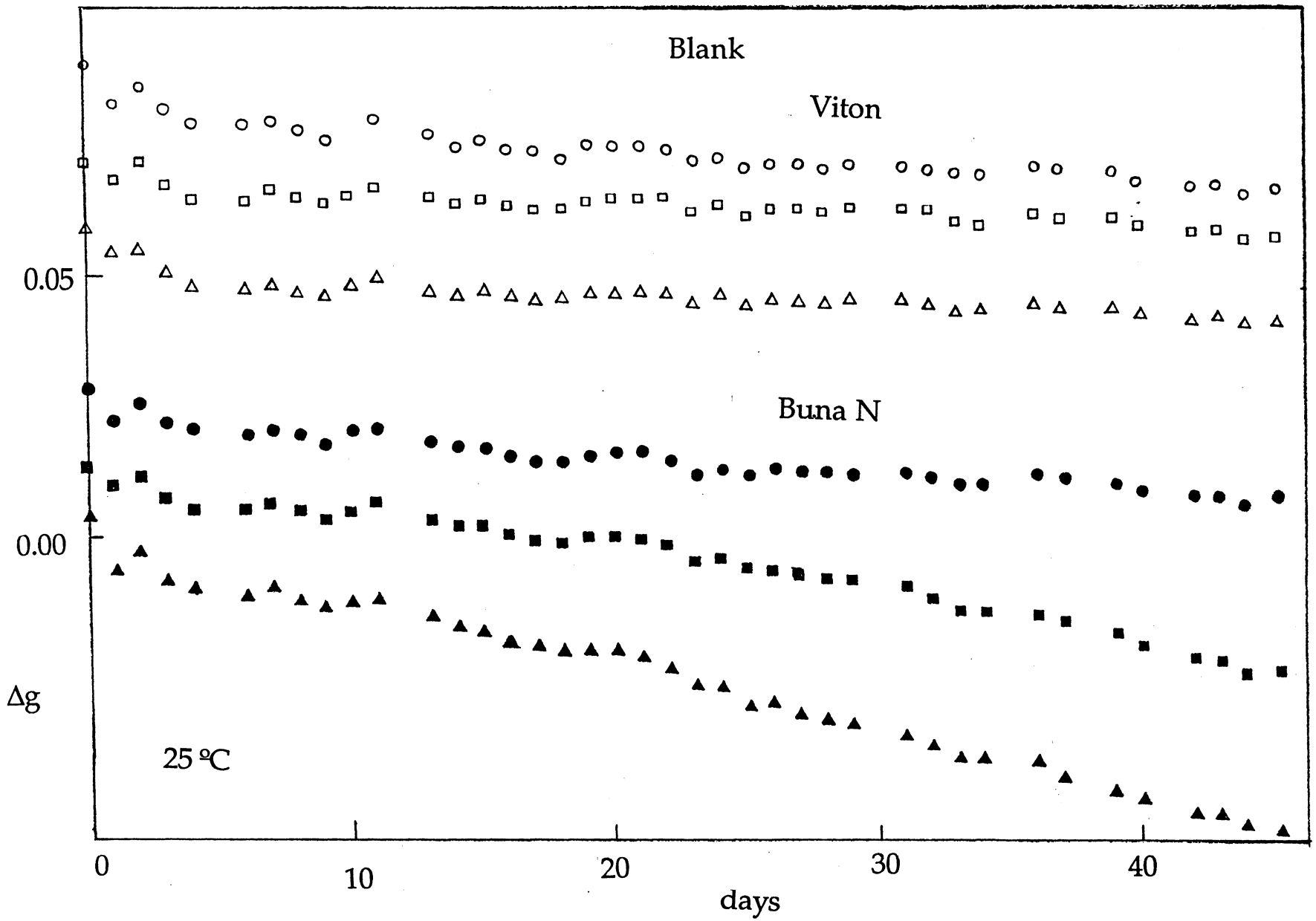

A6. R12 permeation through Viton and Buna N O-rings at room temperature (0.060" grooves). No induction period is apparent.

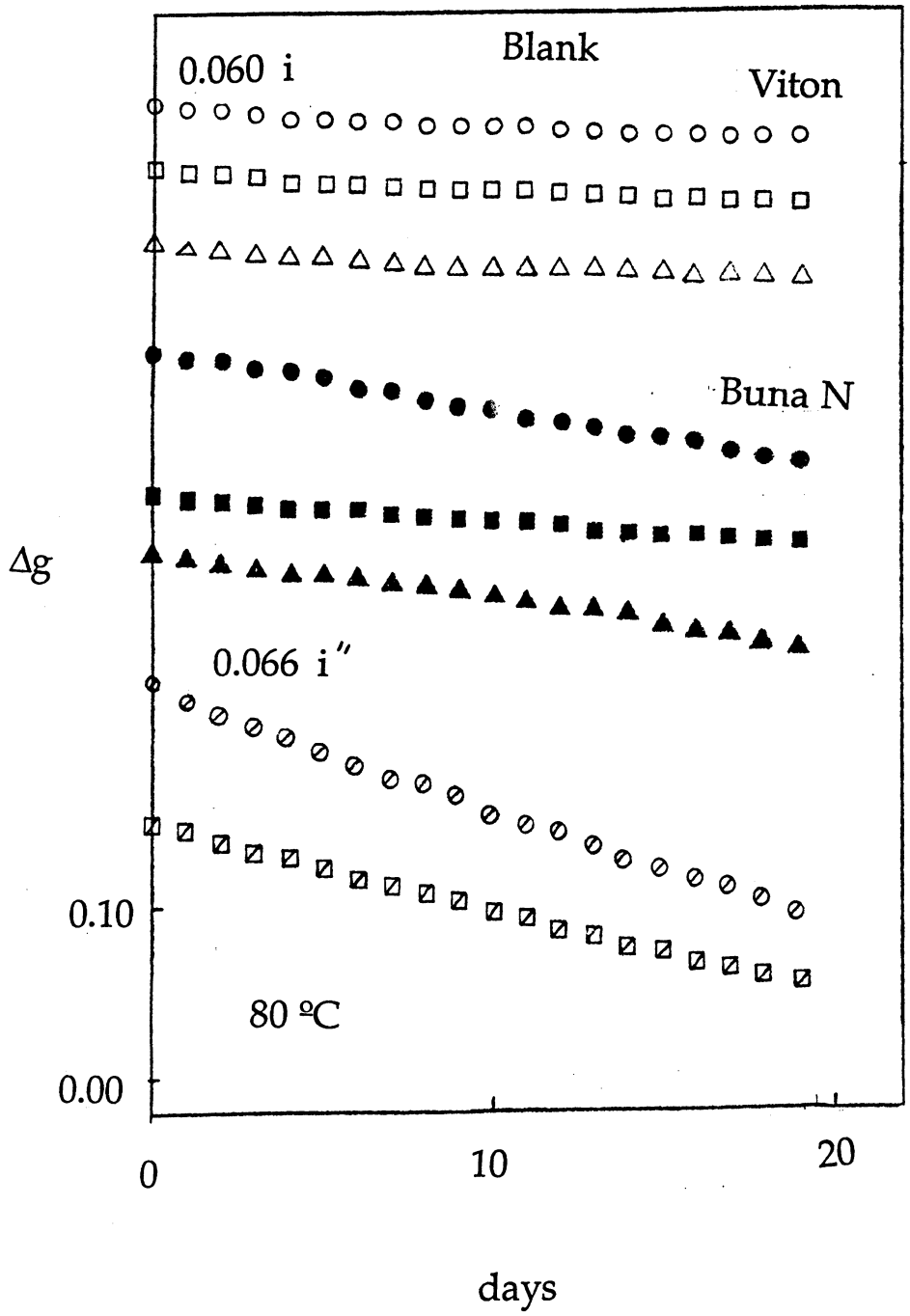

A7. Comparison of R12 permeation through Viton (0.060" groove) and Buna N (0.060" and 0.066" grooves) at 80°C.

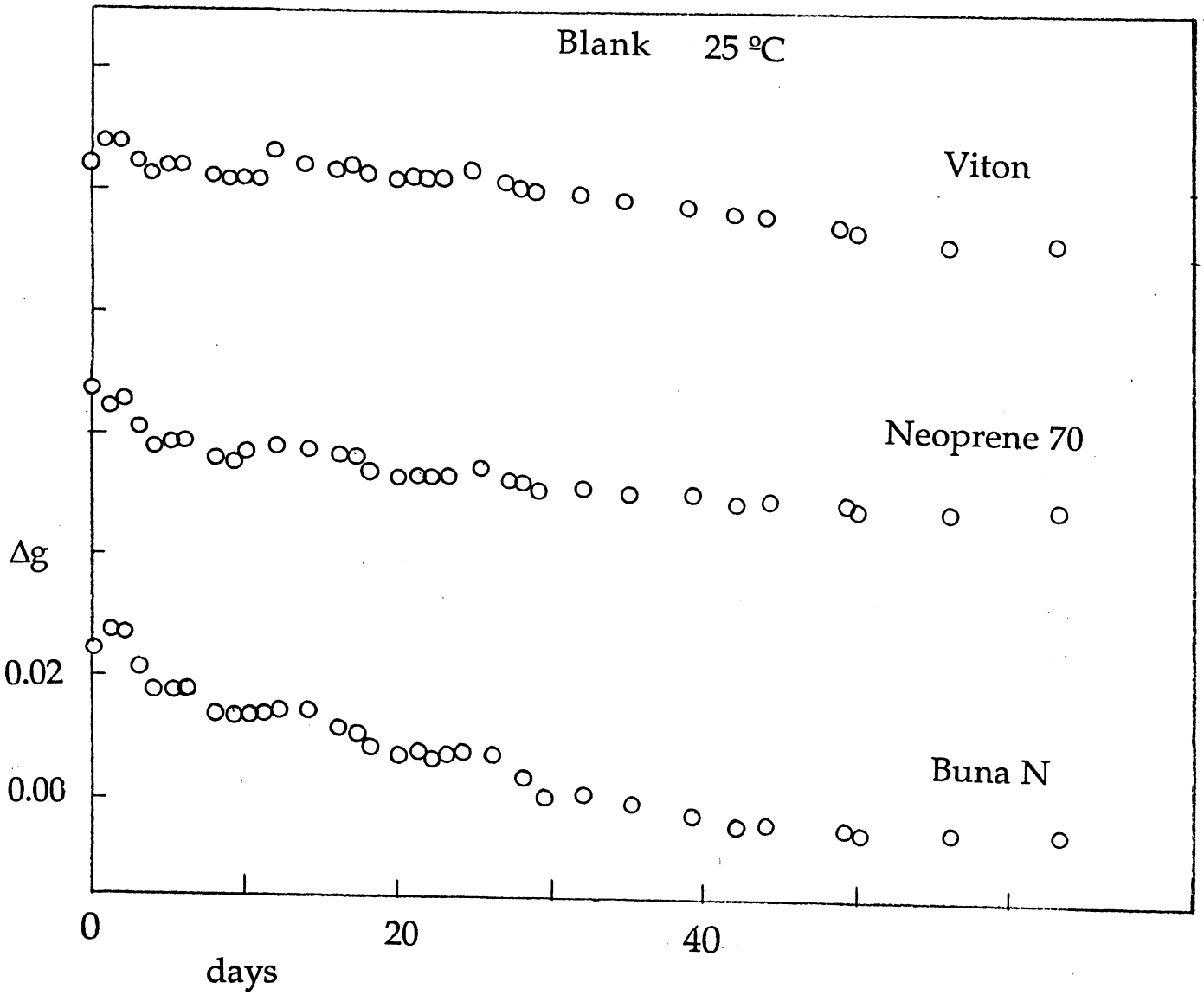

A8. Comparison of 134a permeation at room temperature through Viton, Neoprene and Buna N O-rings (0.060" groove).

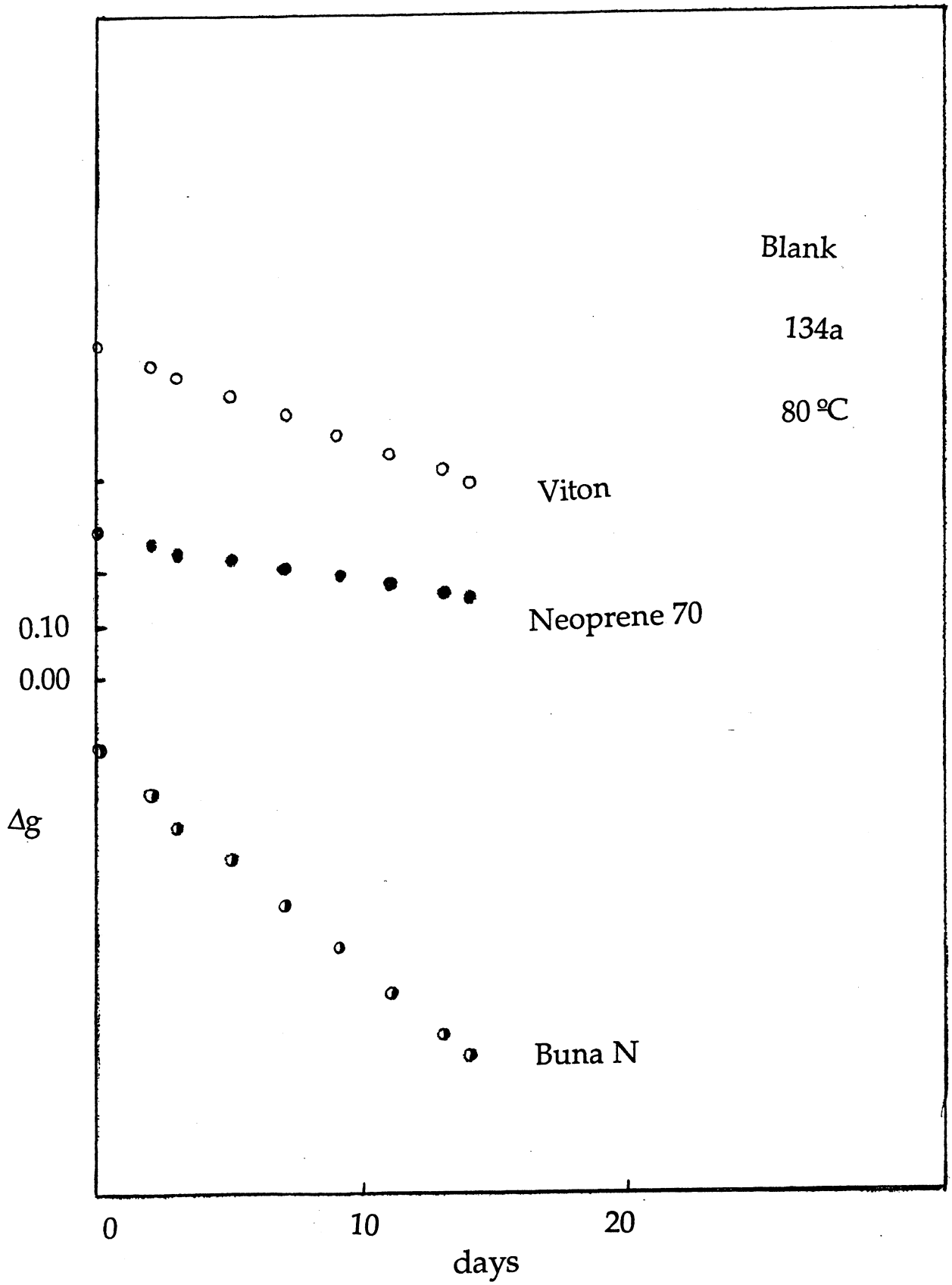

A9. Comparison of 134a permeation at 80°C through Viton, Neoprene and Buna N O-rings (0.060" groove).

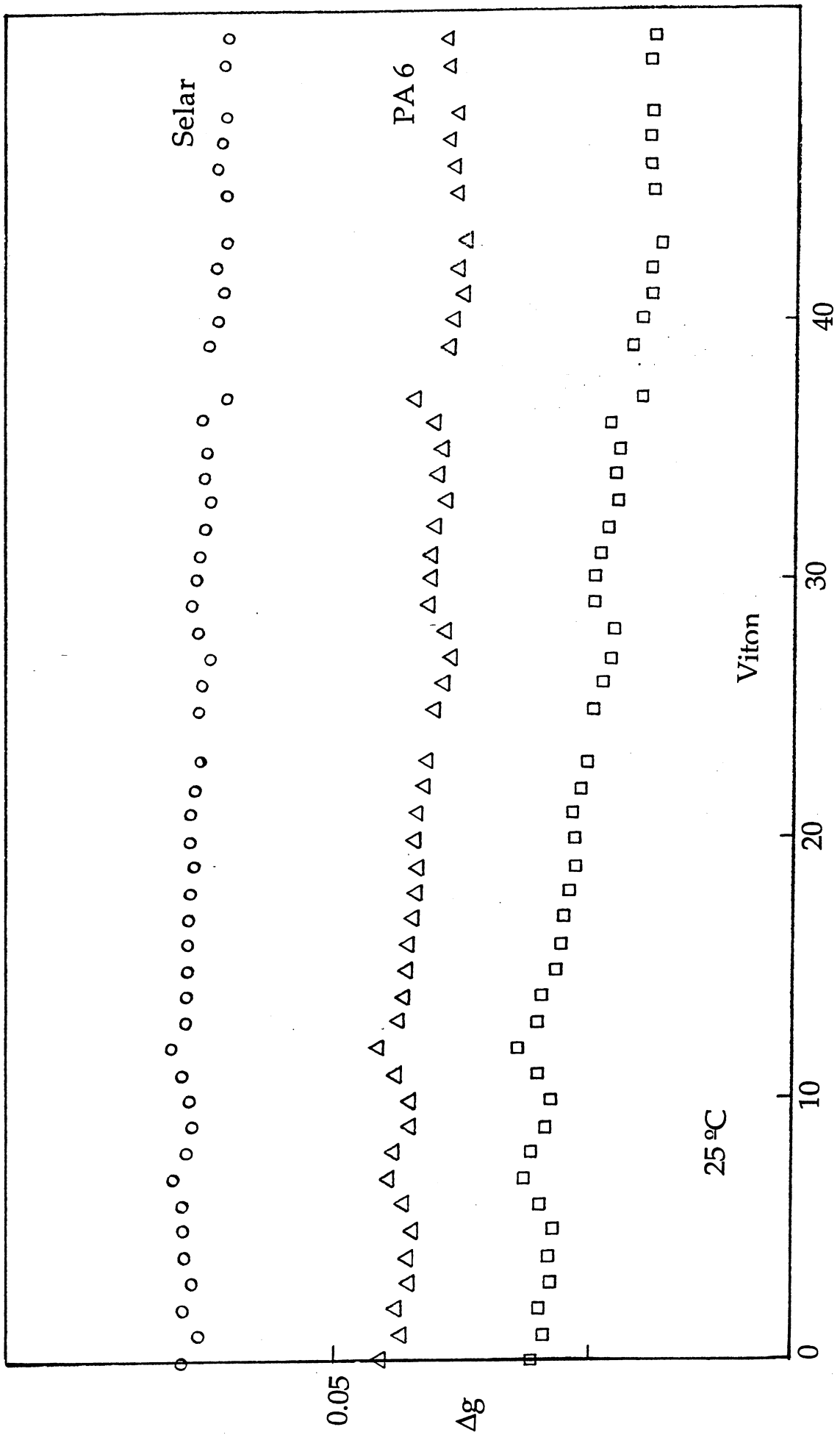

A10. Comparison of R12 permeation through a Selar OH and two nylon 6 (PA6) films at room temperature.

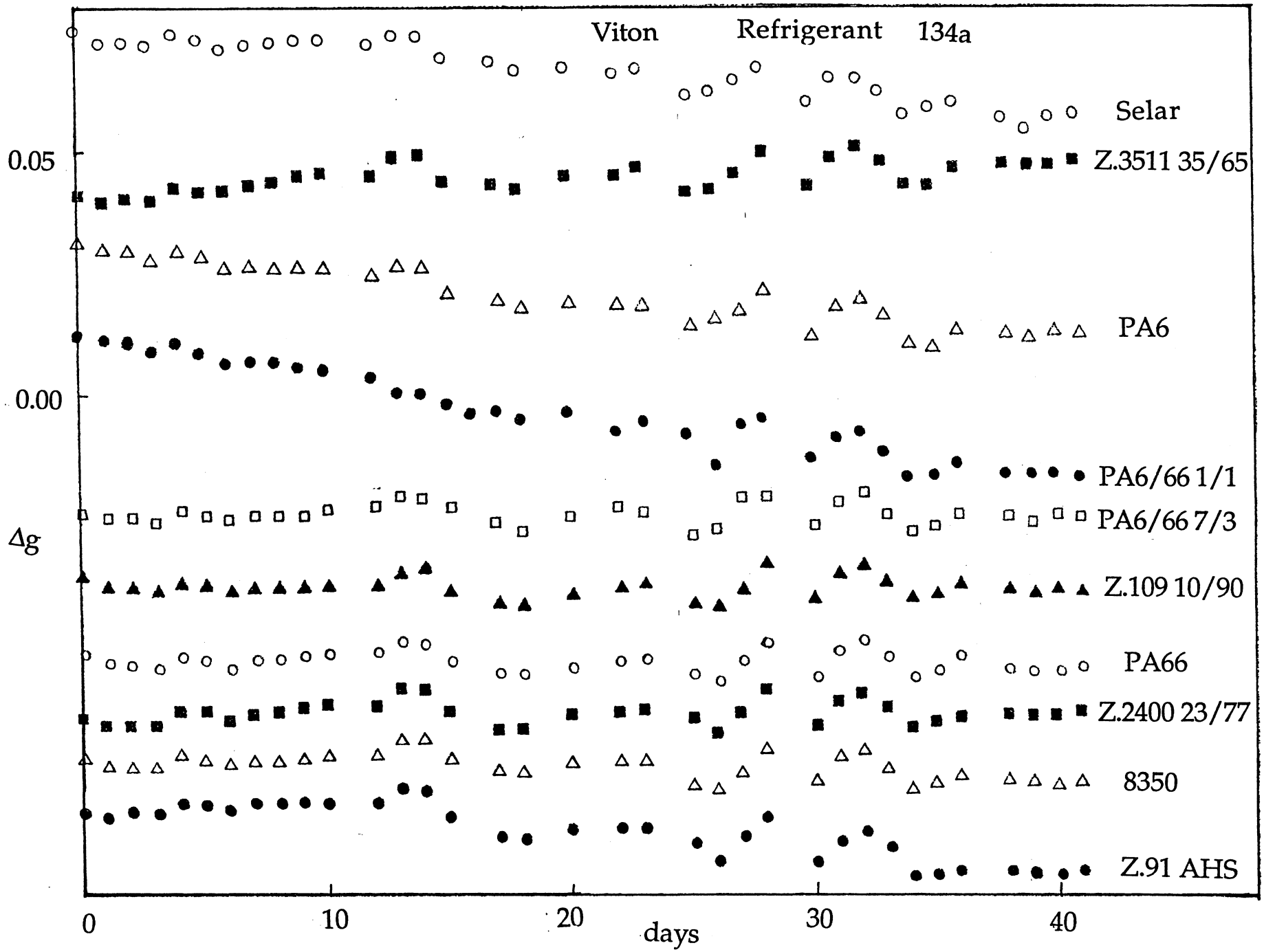

A11. Comparison of 134a permeation through a variety of nylon films at room temperature.

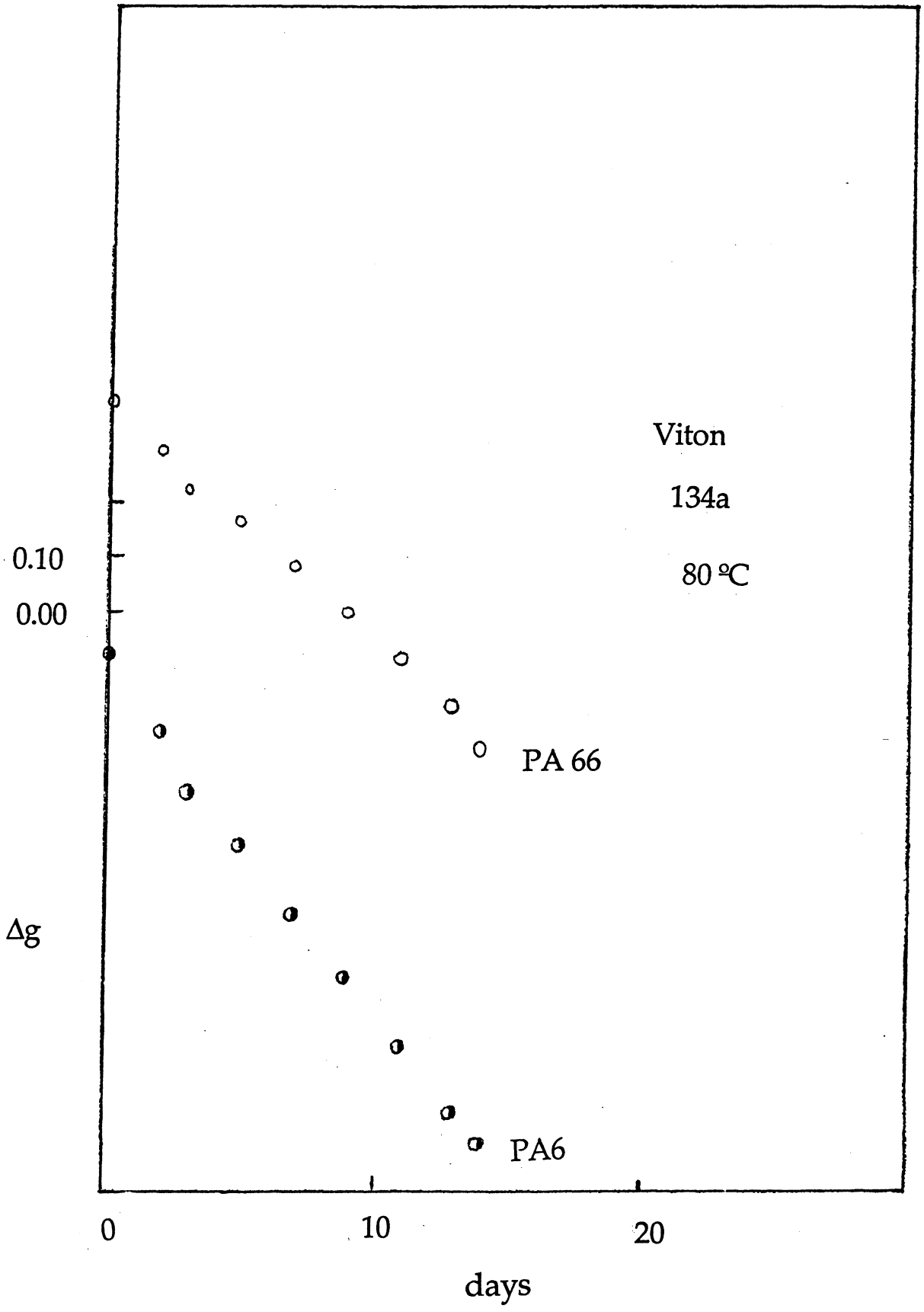

A12. Comparison of 134a permeation through Nylon 6 and 66 films at 80°C.

B. Effects of "Physical" Aging.

1. Objectives and Introduction.

Current engine chamber environments for refrigerant tubing involves temperature up to 200°F (93°C) with 285°F (140°C) environments anticipated as higher engine temperatures are increased for greater efficiency. Short term tests up to 350°F (177°C) have been proposed for tubing qualification. As shown in Part A, refrigerant permeation increases significantly with temperature. An additional problem is the potential for both physical and chemical effects due to the elevated temperatures. Physical aging, in the normally used sense, involves a slow approach of a sample to its equilibrium volume (extrapolated from above the glass transition temperature (Tg)) at temperatures below Tg. This is accompanied by an increase in stiffness. Tg for the nylons used here is ca. 45°C (125°F). In crystalline polymers, however, similar physical aging effects can occur at temperatures above the nominal Tg, attributed to the presence of a "double" or "distributed" Tg which in turn is attributed to the presence of both "wholly amorphous" molecular segments (giving rise to the nominal Tg) and segments constrained by the crystals and therefore requiring a higher temperature for equivalent degrees of molecular mobility. In the polymer PACM-12, a cyclohexyl containing polyamide, we had previously shown physical aging effects up to ca. 50°C above Tg, i.e. well within the temperature range of concern. This part of the research project was directed at investigating the potential of such effects for both the sample tubing materials and some of the blends and copolymers described in Part A. In addition to the physical aging effect due to volume contraction of the amorphous regions, addition effects can occur in the complex tubing compositions due to chemical effects such as transamidation (a chemical reaction changing the sequence structure in copolymers and blends) and degradation as well as physical effects due to

changes in crystallinity. Primary characterization techniques were thermal analysis (measurement of temperatures and heats of melting and crystallization), x-ray diffraction (unit cell and crystallinity characterization) and tensile deformation (modulus and elongation).

2. Experimental

Materials. The majority of the measurements were done with tubing materials supplied by R. Duddleston of Parker Hannifin Corporation. This included 4 granular polyamide blends: Zytel 91AHS and Zytel 726 (hereafter 91AHS and 726) from Du Pont and 8350 and 8358 from Allied (see Table A-II). Besides this we obtained subsequently several hoses made from these or related materials and the copolymers (Table A-III) and blends from DuPont. Compression molded sheets (0.5 and 2 mm thick) with standard thermal history consisting of 5 min. melting at 250°C (5000 psi) and quenching in ice water were prepared from the granules. For aging studies, samples (20 x 10 x 0.5 mm) were wrapped in Al-foil and isothermally annealed at 80-180°C in air and at 100°C in boiling water for 1-10000 min. and examined by differential scanning calorimetry (DSC), optical and electron microscopy, x-ray diffraction, and tensile deformation.

DSC measurements. Discs (6 mm diameter) were punched out from 0.5 mm thick sheets. Heating and cooling curves were measured in the temperature range 50-230°C, at 20°C/min. At least two independent measurements were made for each sample. Melting or crystallization temperatures, shown in Tables, correspond to peak values.

X-ray measurements. A Scintag x-ray goniometer was used for x-ray diffraction in the reflection mode. The Cu K_a radiation was Ni filtered; the detector was

solid state Ge type. Continuous scans between 2θ = 10 and 32° were measured at room temperature at 2°2θ /min. Scans at higher temperatures were done in N_2 atmosphere using the heating stage on the goniometer. The whole set of measurements at elevated temperatures was done with one sample being gradually and stepwise heated (or cooled). After 20 min. temperature equilibration at the desired temperature, a scan was recorded and the temperature then changed.

Tensile deformation. Tensile properties were measured with sheet specimen samples (thickness 0.5±0.05 mm) type IV according to ASTM D638 at room temperature. Five specimens were tested for each condition; results tabulated are averages. The dumbbell shaped specimens had a width of 1/4" and a narrow section length of 1.3".

3. Results and Discussion

Aging of tubing materials followed by DSC.

DSC was chosen for investigation of structural changes due to aging for its advantages: it needs only a small amount of sample and can rapidly and sensitively monitor the changes in melting and crystallization behavior and crystallinity. Before (measuring) aging, all samples received equal thermal history: melting 5 min. at 250°C and quenching in ice water. The initially imposed thermal history, 5 min melting at 250°C followed by quenching resembles the actual manufacturing process of nylon hoses. The samples were aged for periods t_a min. each, differing by an order of magnitude. Our DSC equipment did not allow routine measurements below 50°C and so we were unable to follow changes of T_g. As described in Part A, (see Table A-II), tubing

materials at our disposal are complicated blends containing PA-6 or PA-6/PA-66 copolymers as matrix and rubber impact modifier (polyolefin copolymer) particles or/and plasticizer (n-butylsulfonamide) together with additional small amounts of stabilizers and antioxidants. As it turned out that the rubber used is partly crystalline, we often observed complicated DSC scans containing several peaks due to polyethylene crystalline sequences of the rubber (below 100°C). In addition multiple polyamide peaks in the range 100-220°C were observed. The main results of DSC measurements are summarized in Tables B1-4, where only results concerning melting of the PA component are shown. The results for the PE component are reported later. To give an idea about the changes in shape of the DSC scans we show here in Figs. 1-4 scans of our four tubing materials quenched from the melt in ice water (Q) and annealed 10000 min. at temperatures in the range of 80-180°C in air and in boiling water (100W). The individual materials are discussed below.

91AHS. This tubing material contains only the PA-6/PA-66 15/85 copolymer and about 18% of n-butylsulfonamide plasticizer. The quenched sample has a single broad melting peak (T_{m2}). Due to annealing a second, low temperature peak (T_{m1}) appears. Both peaks T_{m1} and T_{m2} tend to move to higher temperatures in the course of annealing. This trend is illustrated in Fig. 5. The lines on these figures are to aid in the identification of the points, the values shown are, in general, averages of 2 samples which differed by less than 1° for T_{m2}, but by several degrees at times for the annealing peak. As would be expected, the annealing temperature T_a has a marked effect on structural changes. Mainly the T_{m2} values increase by 10-15°C at the highest T_a and t_a. Very interesting is the effect of annealing in boiling water. It exceeds the effect of annealing in air at the same temperature and could be compared to annealing at

180°C in air. It is clear that the interaction of water with PA H-bonds is very important and enables an easier recrystallization. The increase of T_{m1} values is much more dependant on T_a than that of T_{m2}. As in many polymers, it occurs some 20°C above the annealing temperature. As can be seen, by comparing the ΔH_{m1} and ΔH_{m2} values in Table 2, the extent of the lower melting material is less than 10% of the higher melting material; in other polymers it is attributed to material crystallizing at the annealing temperature and likely is the explanation here also. Figure 6 shows that, along with melting temperatures, the crystallinity of the sample 91AHS also increases, as is indicated by the ΔH_m values (heats of fusion of both T_{m1} and T_{m2}).

726. This material is a blend of PA-6 with polyolefin copolymer. Due to the homopolymer nature of the PA-6 component, the T_m values are generally higher than that of 91AHS. The presence of rubber modifier is responsible for low temperature melting peaks in Fig. 2. The PA melting is again characterized by low and high temperature peaks with 3 peaks superimposed in the samples of lower T_a: a broad T_{m1} is seen in the quenched sample, with a sharper "annealing peak" superimposed in the annealed samples, again 20°C above T_a. At T_a=160°C and longer t_a we have observed, also, smaller very high melting peaks. Figure 7 shows the changes of melting peaks with T_a and t_a. In contrast to 91AHS, we see that T_{m2} values tend to slightly decrease or remain unchanged as a function of T_a and t_a. The low melting material (T_{m1} only seen for ta > 1 min) tends to increase with increasing T_a and t_a. Crystallinity, characterized by ΔH_m values (Fig. 6), follows the trend of T_{m2} values.

8350. The composition of this tubing material is similar to 726 and similar also are its aging characteristics. T_{m2} values, mainly at higher T_a, tend to decrease,

but the T_{m1} values have the opposite tendency (Fig. 8). Except for T_a=180°C, the ΔH_m values tend to decrease slightly at longer t_a values (Fig. 9).

8358. This is a complex blend composed of PA-6/PA-66 85/15 copolymer, polyolefin copolymer (37%) and 5% of n-butylsulfonamide plasticizer. This composition results in relatively low T_m values, as can be seen in Table 4 and Fig. 10. Here, both T_{m2} and T_{m1} values increase with increasing T_a and t_a. The same trend may be traced in crystallinity, characterized by ΔH_m values (Fig. 9). Again, we may notice a marked effect of annealing in water on the growth of T_{m2} and T_{m1} values. A complex low temperature DSC trace is observed for annealing at 100°C in air or water; this is at least in part due to the polyolefin.

Rubber peaks. The samples 8350, 8358 and 726 contain rubber particles that are partially crystalline. Their crystallinity may change during annealing below their melting temperature (~90°C). Therefore we show here only the data measured at T_a=80°C (Fig. 11). Annealing at higher temperatures caused the PE crystals to melt and then reappear during cooling to room temperature. This situation was the same for all samples annealed above 100°C temperatures and thus the resulting PE structure did not differ much from that of the original quenched samples. The DSC results for PE melting in such cases were practically identical and are not shown here. As shown in Figs. 2-4 and Fig. 11, there are two or three melting peaks which most probably represent the melting of PE crystalline copolymer sequences of various lengths. The higher melting peaks tend to increase linearly with log t_a. Also the PE crystallinity tends to increase with t_a, except for 726, as follows from the ΔH_m values in Fig. 11. Annealing at 100°C results in apparent polyolefin peaks above 100°C for the Allied material but not the Zytel 726; presumably a different polyolefin is involved.

Time-temperature superposition. In spite of some scatter of the experimental data, possibly due to local differences in the blend composition and relatively small sample size, we tried to apply the time-temperature super-position principle to the DSC results to permit prediction of effects over larger periods of time . This is normally used to predict long term mechanical properties; we do not know of its use before for thermal effects. An 80°C reference T_a was used. Except for the sample 726, where the scatter was too high, we were able to get reasonable plots in which the data could be placed on a single curve by shifting the measured points along the time axis. This is shown in Figs. 12-15. All 3 samples have two features in common: the overall crystallinity (ΔH_m values) and T_{m1} values tend to increase during aging. The main, high temperature peaks (T_{m2} values) increase markedly only in the copolymer samples 91AHS and 8358. The increase of the low temperature melting peaks differs in all 3 samples. Sample 8350 exhibits a relatively moderate Tm1 increase and its time axis could be matched to that of the T_{m2} and ΔH_m values. However, in samples 91AHS and 8358, the increase of T_{m1} values with t_a is much higher (almost 100°C), but it proceeds much more slowly than in 8350 (note the different time scales). Both 91AHS and 8358 are PA-6/PA-66 copolymers. Since T_{m1} is presumed to be due to melting to crystals formed at T_a it is obvious that to reorganize the structure in a random copolymer in order to put together longer common PA sequences, making it possible to form large and higher melting crystallites, takes much more time than in a homopolymer. Similar curves presumably could be used to predict changes in T_m and ΔH_m with t_a for any T_a, involving only a shift in the log t_a axis.

Homopolymers and blends. DSC measurements were also made on PA6, PA66 and several blends, as a function of T_a and t_a. For PA6 (T_m = 217°C, 423°F) annealing at 140°C (238°F) and above yielded an "annealing peak", i.e. some of the amorphous material crystallized at the annealing temperature (Table B5). This was also seen for the PA6 sample annealed in boiling water, $T_m(a)$ being a sharp peak at about 175°C. The main melting peak remained nearly constant in position and area, the change in T_{m2} (decrease) and ΔH_m (increase) for annealing at 180°C (356°F) and 100°C in water being due to the overlapping of a large $T_m(a)$ peak. For nylon 66, having a T_{m2} of 260°C (500°F), annealing at temperature of 180°C or less had essentially no effect other than for the development of the $T_m(a)$ peak.

The DSC curves (for t_a=104 min.) and plots of T_m vs t_a for a nylon 6/66 7/3 blend are shown in Figs. 16 and 17. The annealing peak $T_m(a)$ is clearly seen for annealing temperatures above 140°C, merging with the T_m(PA6) peak for 180°C annealing. At 160°C the behavior is complex, the PA66 peak being greatly disturbed. In general there appears to be no change in the interaction of the two components with t_a; the T_m of both components, however, are lowered by nearly 10°C by the presence of the other (see Part C). Annealing in 100°C water is seen as previously, to yield a significant increase in T_m.

X-ray measurements of aged samples. From x-ray goniometer scans, measured at room temperature with quenched and annealed samples, the intensities of the diffraction peaks and the intensity at $2\theta \doteq 21.5\text{-}22^\circ$ which is proportional to the amorphous diffraction, were evaluated. In the diffraction scans 2 or 3 peaks and the minimum at about $2\theta = 22^\circ$ could be found eventually if the annealing time was sufficiently long. The diffraction peaks at approximately 4.4 and 3.8 A (20 and 23° 2θ) correspond to the polyamide α-modification and the peak at about

4.2Å (21°2θ) belongs to the PA γ-modification. Simultaneously, at 4.2Å, lies also the PE peak of the polyolefin copolymer. The 2θ positions of the peaks did not change significantly during aging, only the relative intensities changed for individual peaks. Sometimes the peaks were not clearly resolved, this is marked by s (shoulder) in the respective Tables. In samples of low crystallinity, where the minimum between 4.4Å (or 4.2Å) and 3.8Å peaks did not form, the intensity at 2θ=22° is indicated in parentheses.

Some examples of x-ray diffraction patterns, showing samples quenched (Q), annealed 10000 min. at 100°C in water (100W) and 180°C in air, are presented in Figs. 18-21. The results of all x-ray measurements of annealed samples are summarized in Tables 6-9. In accord with DSC measurements, the x-ray data confirm that even the samples quenched in ice water are partially crystalline: 8350 and 726 (homopolymers) in the α-modification and 91AHS and 8358 in the γ-modification. The well annealed samples are characterized by peaks belonging to the α-modification. The samples 726, 8350 and 8358 have also a 4.2 Å peak which is due to polyethylene crystallites from the polyolefin copolymer. This was proven by measurements at temperatures above 100°C where this peak, present at 25°C, disappeared. The PE peak complicates the situation in attempting to measure the PA x-ray crystallinity. In low crystallinity samples with a higher γ-content, it is not possible to find in the x-ray diffractogram a reliable 2θ position which would correspond solely to amorphous scatterings. To get at least some idea about crystallinity changes during aging, we have adopted an index %A which represents the ratio of intensities of the "amorphous" minimum at 2θ=22° and average intensity of crystalline peaks present. The results are shown in Fig. 22. In spite of considerable scatter, there is a clear tendency to decrease the %A during aging. The plots are comparable to similar plots of ΔH_m values.

X-ray measurements at higher temperatures. The heating stage of the x-ray goniometer made it possible to investigate changes in the x-ray diffraction spectra at higher temperatures. Samples slowly cooled from melt to room temperature were used for such measurements. In order to assess the possible influence of the plasticizer in the 91AHS sample we have extracted the plasticizer by boiling xylene. As shown in Figs. 23 and 24, the presence of the plasticizer did not affect the 2θ position or temperature changes of the diffraction spectrum of 91AHS. The plasticizer is located evidently only in the PA amorphous phase (and thus affecting the permeation properties as shown in Part A). As Figs. 23 and 24 show, the structural changes due to temperature slightly differ from sample to sample. The tubing materials based on PA-6 homopolymer (726 and 8350) have a lower tendency for the α–γ transition, because their principal α-peaks do not merge to single γ-peak at temperatures above 150°C. The γ-peak (at about 2θ=21°) in 726 disappears below 100°C and does not appear at all during cooling to room temperature. In the sample 8350 the γ-peak persists during heating, besides α-peaks, up to the melt and reappears during cooling below 100°C. Sample 8358 has both α and γ-peaks during heating and cooling and it undergoes the well known α–γ transition above 150°C both in heating and cooling. The γ-peak is always present in this sample. Sample 91AHS, original and extracted, both undergo the α–γ transition between 100-150°C, during both heating and cooling, but never shows the low temperature γ-peak. All this confirms the assumption that in polyamides there are two γ-modifications. One is stable at temperatures above 100°C and results from α→γ recrystallization (γ_{HT}). The other γ-modification forms by fast cooling from the melt (γ_q). It is unstable and above 100°C transforms to the stable a-modification.

Morphology. Our research was aimed at determining the best conditions for revealing the internal structure of tubing materials on the electron microscope resolution level. We have tried various alkali reagents (NaOH, KOH, NH_4OH, n-butylamine, n-amylamine) at various concentrations and temperatures, and diluted (~10%) HCOOH, for selective etching of polyamide materials. No entirely satisfactory results were obtained with any reagent tested. The best results were observed using 15-20% KOH water solutions at 8--100°C for 10-20 hours. The main problem is that our tubing materials are of low crystallinity and the crystallites are far from perfect. The presence of other blend components complicates the situation but is revealed by the etching; with pure PA-6 or PA-66 the lamellar spherulitic morphology could be easy detected by selective etching using 15-20% KOH water solution at 80-100°C.

Mechanical property measurements. The modulus and elongation at failure for compression molded films of the 4 tubing materials (Table AI) are listed in Table B10. The high modulus of 8350 suggests it does not contain plasticizer whereas 726 likely does. If so, then annealing in 100°C water is seen to raise the modulus of all 3 plasticized samples (particularly that of 91AH5), possibly due to some plasticizer extraction as well as increases in crystallinity. Annealing at 160°C is seen to drastically reduce the elongation of the two nylon 6 materials (8350 and 726), while not affecting that of the two copolymers within the limits of the elongation attainable with our instrument. This we relate to the increase in crystallinity of PA6 with annealing as evidenced by the development of the annealing peak.

4. Conclusions

The primary effect of aging at elevated temperatures, as it would affect room temperature properties, is the development of the annealing peak, $T_m(a)$, indicating the crystallization of a portion of the "amorphous" material, and a change in crystal structure of the nylon 6 containing materials (91AHS, 8358 and, presumably, blends $\gamma_q \rightarrow \alpha$). The x-ray measurements, in addition, show a conversion, generally reversible, of α to γ_{HT}, at elevated temperatures but temperatures well within the maximum use temperature proposed (285°F, 140°C) for the copolymers. These changes suggest caution is needed in the application of PA6 and 6/66 copolymers at the proposed temperature and, in particular, indicates that using short term tests at 355°F (177°C) are inappropriate; the physical state of the material will have been changed, a change which would not necessarily have occurred for longer times at lower temperatures.

Those materials containing polyolefin likewise present problems, the crystalline sequences in the polyolefin melting near 100°C and also undergoing annealing effects. It is noted that there is no evidence for either the normal physical aging (decrease in free volume in "amorphous" regions) or chemical aging (degradation) in these experiments.

T_{a1}°C	t_{a1}min	T_{m1}°C	ΔH_{m1} cal/g	T_{m21}°C	ΔH_m, cal/g
0	0			205	11
80	1			202.4	12.2
80	10			203.5	12.5
80	100	98.5	0.6	205.3	11.2
80	1000	102.4	1	205.6	12
80	10000	102	1	202.8	12.9
100	1			203	11.7
100	10	106		202.3	12.3
100	100	112.8	0.8	204	11
100	1000	113		203.5	16.5
100	10000	120		203.3	15
100W	1			205.2	15
100W	10	165		206.9	17.1
100W	100	177		209.5	20.6
100W	1000	162		214.4	23
100W	10000	165		216	25.8
120	1			204.9	9.5
120	10	124.4	0.5	205	9.5
120	100	130.8	0.8	205	9.3
120	1000	136.3	0.9	205	12.5
120	10000	146		209	15
140	1			204.6	12.5
140	10	148		205.4	11.8
140	100	150		205.3	13.3
140	1000	157		205.2	13.8
140	10000	173		211.5	15.4
160	1			205.5	10
160	10	168		205	11.8
160	100	172		204.3	12.4
160	1000	178		206.3	15
160	10000	191		211.9	15
180	1			204.8	11.1
180	10	188		204.5	12
180	100	155 188		207.5	13.7
180	1000	150 201		209	19
180	10000	210		219	20.7

B1 Results of DSC measurements of aging; 91AHS

T_{a1}°C	t_{a1}min	T_{m1}°C	ΔH_{m1} cal/g	T_{m21}°C	ΔH_m, cal/g
0	0	146.7	3	219.4	10
80	1	149	1.2	217.5	8.8
80	10			217	8.2
80	100	158	1.6	218	6.7
80	1000	168	0.8	217.2	8
80	10000			217.1	8
100	1			217.2	8.5
100	10	110-180	0.5	218	7.7
100	100			218.2	10
100	1000	110-170	2	217.2	7.0
100	10000	110-170	2	216.2	7.5
100W	1	157	3.5	218	11
100W	10	160	2.2	218.3	10.6
100W	100	169	4.2	218.2	11
100W	1000	172	2.2	218.1	11.3
100W	10000	175	1.9	217	10.6
120	1	170.2	0.9	216.1	8
120	10	124	2.9	218.7	9.8
120	100	130.5	1.5	217	8.2
120	1000	137.4	1.8	218.2	8.1
120	10000	145	2.5	218.3	8.5
140	1	162	2.5	218.4	9.2
140	10	147	3.5	218.9	10.2
140	100	153	2	219	8.6
140	1000	156	4.5	218.5	10.9
140	10000	160	3.2	217.5	9.6
160	1	153	3.5	218.8	10.2
160	10	165.5	4.9	219.1	11.5
160	100	170		218.3 226	7.3
160	1000	172.5		218 226	7.6
160	10000	184		217.3 225	8.5
180	1	152.7	0.5	216.6	8
180	10	176.5	2.1	217.4	10.4
180	100	186.5	2.5	217.8	8.8
180	1000	198		218.4	8.9
180	10000	192		219	10

B2 Results of DSC measurements of aging 726; PA peaks

T_{a1}°C	t_{a1}min	T_{m1}°C	ΔH_{m1} cal/g	T_{m21}°C	ΔH_m, cal/g
0	0	172	3.4	218.4	13
80	1	166	2.6	217	13
80	10	167	2.6	217	13.6
80	100	167		217	13
80	1000	172		217.5	13
80	10000	174		218	12.7
100	1	168		217.6	13.2
100	10	179		217.7	12.9
100	100	180		217.6	12.8
100	1000	185		217.4	11.7
100	10000	185		217	10.8
100W	1	165	5	217.4	14.9
100W	10	165	6	218	15.3
100W	100	169	5.8	218.4	15.6
100W	1000	174	4.8	218.5	14.4
100W	10000	176	3.8	218.3	13
120	1	170	4.7	217.8	14.6
120	10	168	3.9	217.3	14.4
120	100	166	3.8	217.9	13.4
120	1000	166	3.6	217.8	12.9
120	10000	145.6	3.2	217.4	13.5
140	1	172	3.7	218.2	13.7
140	10	143	4.8	218.2	15
140	100	154	2.5	218.1	13.2
140	1000	156	2	217.9	12.4
140	10000	165	2	216.7	12
160	1	170	3.9	218	14
160	10	165	4	217.8	14.7
160	100	171	3.3	217.5	13.6
160	1000	178	2.9	217	15
160	10000	197		214.7	14.5
180	1	175	2	217.8	13.1
180	10	182	5	217.2	15.5
180	100	187		216.5	17.7
180	1000	197		215.8	18.9
180	10000	199		214	19

B3 Results of DSC measurements of aging 8350, PA peaks

T_{a1}°C	t_{a1}min	T_{m1}°C	ΔH_{m1} cal/g	T_{m21}°C	ΔH_m, cal/g
0	0			193.2	7.4
80	1			192.8	8.7
80	10			192.8	8.2
80	100			192.4	8
80	1000			193	8.1
80	10000			194	7.7
100	1	96.3	0.4	193.5	7.6
100	10	104	0.53	194	7.8
100	100	105	0.36	194	7.8
100	1000	108	0.24	193.6	9.8
100	10000	110	0.53	197	9.7
100W	1	102		193.9	7.8
100W	10	104		195.7	9
100W	100	105	0.4	197	11.5
100W	1000	105 109		197.2	12.6
100W	10000	112.5	0.5	199.5	12.9
120	1			191.4	7.7
120	10	123.3	0.5	192.1	8.2
120	100	130.3	0.8	194	8.7
120	1000	134.5	0.9	192.6	8.4
120	10000	137	1	193.5	7.7
140	1	114	2	194.7	8.1
140	10	151		194	8.5
140	100	154		194.3	8.5
140	1000	158		192.7	8.9
140	10000	167		194 212	13.1
160	1	162		195	7.4
160	10	168		194.8	9
160	100	173		195.4	9.5
160	1000	177		196	10.4
160	10000	183.5		198	12.3
180	1			194	8.3
180	10	186		194	10
180	100	189		196	10
180	1000	185		196	11.8
180	10000	184		198	11.7

B4 Results of DSC measurements of aging 8358; PA peaks

T_{a1} °C	t_a min	T_{m1} °C	ΔH_{m1} cal/g	T_{m2} °C	ΔH_{m2} cal/g
0	0	136.3	7.3	216.7	14
80	1	136	8.6	214.8	14.2
80	10	135	9.6	215.4	15.7
80	100	137.1	6.1	214.7	14.1
80	1000	134.1	9.2	215.7	15.6
80	10000	127.9	17.7	217.5	16.6
100	1	143	2.5	215.1	15.4
100	10	99.6,150.7*	0.3, 1.3	215.6	15.6
100	100	101.1, 149.0	0.4, 1.4	215.0	15.6
100	1000	105, 140.7	--	216.3	--
100	10000	116.5 --	3.2	216.9	17.6
* two broad peaks seen					
100W	1	163.3	0.9	216.6	14.7
100W	10	174.6	0.3	218.2	13.4
100W	100	178.0	0.3	219.0	13.3
100W	1000	178.0	0.4	216.4	16.*
100W	10000	179	0.5	216.8	18.1
*including T_{m1}, peaks overlap					
120	1	145.7	0.85	214.8	14.7
120	10	130.7	2.4	215.6	15.6
120	100	120.7	4.2	215.0	14.6
120	1000	138.7	5.6	218.4	17.0
120	10000	140.8	1.6	216.1	17.5
140	1	127.5	3.5	215.5	15.2
140	10	154.5	4.5	214.6	14.6
140	100	150.7	4.8	216.3	16.0
140	1000	159.2	5.3	213.9	17.4
140	10000	163.0	1.5	216.4	16.2
160	1	--	--	--	--
160	10	164.6	1.0	216.4	16.1
160	100	173.1	1.2	216.2	15.7
160	1000	180.0	1.4	215.8	15.1
160	10000	179.0	1.4	216.4	15.2
180°	10	161.9	4.8	215.5	14.9
	2140	195.0	4.7	213.7	18.8†
	10000	198.0	6.1	214.8	21.7†
† including T_{m1}, overlapping peaks					

B5 Results of DSC measurements of aging homopolymer PA6

T_{al}°C	t_{al}min	4.4Å, cm*	4.2 Å, cm	3.8 Å, cm	Am, cm
0	0	7.4s	7.4		(6.1)
80	1	8.8	7.8	5.3	(6.6)
	10	8.4	8.4		(6.5)
	100	7.4s	7.6		(5.9)
	1000	8.1	7.7		(6.8)
	10000	8.7	8.9		(6.5)
100	1	8.4s	8.9	4.3	(7.5)
	10	7.8s	9	5.8	(7.1)
	100	7.9	7.7s	3.6	(6.2)
	1000	8.4	8.9	4.4	(7.6)
	10000	6.4	5.5	9.4	3.8
100W	1	8.8		5.3	4.5
	10	8.3		4.7	3.2
	100	9.3		5.5	3.3
	1000	9.3		5.6	3.4
	10000	9.3		5.5	3.3
120	1	8.5s	9.5	4.2s	(6.2)
	10	7.8	7.7s	7	6.9
	100	8	7s	3.7s	(6.5)
	1000	6.8s	6	5.4	5.4
	10000	7.7	7.8	6.9	6.5
140	1	7.1	7.1	4.9	(5.7)
	10	8.5	6.1s	5.7	5.4
	100	5	3.8	3.5	3.2
	1000	7.8	7.7s	6.2	6.1
	10000	8.5	6.8s	7	6.3
160	1	7.2s	7.8	4.7s	6.0
	10	8.5	—	6.2	5.7
	100	8.2	—	6.3	5.3
	1000	7.8	—	5.2	4
	10000	9.4	—	6.8	5
180	1	7.3	—	6.9	6
	10	8.5	—	5.7	3.8
	100	8.7	—	5.7	4
	1000	7.8	—	6	3.7
	10000	9.2	—	7	3.9

*** height of peak on graph**

B6 X-ray peak intensities for aged 91AHS. Am is height of amorphous minimum; ( ) indicates no clear minimum; s indicates the "peak" is only a shoulder

T_{a1}°C	t_{a1}min	4.4Å, cm	4.2 Å, cm	3.8 Å, cm	Am, cm
0	0	8.0s	7.9s	6	5.4
80	1	7s	8.1	5s	(5.5)
	10	7.9s	8.5	5.1	5
	100	6.8s	8.6	4.5s	(5.1)
	1000	8.6	8.8	5.8	5.5
	10000	7.3	9.1	4.7	(5.2)
100	1	8.7	8.6	6.1	5.2
	10	8.7	9	6.1	5.6
	100	8.2	8.2	5.3	5
	1000	8	8.3	5.7	5.4
	10000	7.4	8.2	5	(5.5)
100W	1	7.7	7	5.3	4.2
	10	8.5	8	5.7	5
	100	7.9	7.1	5.4	4.3
	1000	9	8.7	5.8	5.4
	10000	8.4	7.3	5.6	4.3
120	1	6.5s	7.8	3.8s	(4.5)
	10	7.4s	8.1	5.3s	(5.9)
	100	8	8.2	5.3	5.1
	1000	8.2	7.7	5.6	5.2
	10000	7.4s	7.9	5.4	5.1
140	1	6.2	7.9	4.5	(5)
	10	7.2s	8	5.2s	(5.5)
	100	8.2	7.6	5.4	5
	1000	8.2	9.2	5.7	5.5
	10000	8.5	8.2	5.9	5.3
160	1	7.2s	8	5s	(5.3)
	10	7.1s	7.7	4.8s	(5)
	100	7.6	8.4	5.3	(5.5)
	1000	8.2	8.3	5.4	5.4
	10000	8.9	8.7	7.1	5.4
180	1	7.6s	7.9	5.1	(5.2)
	10	7.9	8.5	5.2	(5.5)
	100	7.5	8.3	5.1	5.1
	1000	8.5	8.3	5.8	5.4
	10000	8.9	8.7	7.1	5.4

B7 X-ray peak intensities for aged 726

T_{a1}°C	t_{a1}min	4.4Å, cm	4.2 Å, cm	3.8 Å, cm	Am, cm
0	0	7.3s	7.6	4.8s	(6.1)
80	1	6.8s	9.4	5.5s	(5.5)
	10	5s	8.6	4.3s	(4.3)
	100	5.7s	8.8	4.9s	(4.9)
	1000	5.7s	9	4.7s	(4.7)
	10000	5.4s	8.8	4.4s	(4.5)
100	1	7s	9.2	5.3s	(5.7)
	10	7.1s	8.8	5.9s	(6.5)
	100	7.8	7.5	5	4.5
	1000	9	7	6.1	4.3
	10000	8.7	7.2	5.9	3.4
100W	1	8	6.7	4.6	4.6
	10	8.3	5.6	5.3	3.6
	100	9.4	5.7	5.8	3.7
	1000	8.8	6.6	5.5	3.8
	1000	9.1	6.1	5.7	3.6
120	1	6.7s	8	3.2s	(4.8)
	10	7.3s	8.2	5.7s	(5.8)
	100	8s	8.2	6.1s	(6.1)
	1000	7.6s	8.2	6.1	5.9
	10000	6.6	6.5	4.8	4.1
140	1	7.9s	7.9	5s	(5.8)
	10	7.4	6.9s	5.1	4.8
	100	8.5	8s	6.1	5.9
	1000	7.9	6.8s	5.7s	(5)
	10000	7.7	6.7s	5.9	4.7
160	1	8	6.4s	5.1	4.2
	10	8.8	6.5s	5.9	4.3
	100	8.5	6.1	5.5	4.3
	1000	8.2	5.4s	5.5	4.1
	10000	8.4	6	6.3	4
180	1	8.1s	8.7	6.1s	(6.3)
	10	7.8	5.8	5.6	4
	100	8.1	6.1	5.4	4
	1000	8.9	5.9	6	3.7
	10000	8.4	5.5	5.5	3.6

B8 X-ray intensities for aged 8358

T_{al} °C	t_{al} min	4.4Å, cm	4.2 Å, cm	3.8 Å, cm	Am, cm
0	0	9	8s	8.4	6
80	1	8	7.8s	6.6	5.9
	10	8.2	8.8	7.3	5.5
	100	8.2	9.5	7.3	5.9
	1000	8s	9	6.7	5.7
	10000	7.8	8.8	7.3	5.5
100	1	6	5.9	9.1	4.4
	10	6.7	6.8	8.9	4.7
	100	9.2	9.6	8.1	6.4
	1000	7.1	7	9.2	4.9
	10000	7.8	8.2	6.9	5.7
100W	1	8.7	7.9	8.4	5.4
	10	8.3	7.1	8.7	5
	100	9.1	7.1	7.2	4.8
	1000	9	6.8	9.8	4.7
	10000	6.4	5.4	9.3	3.7
120	1	8.5	8.7	7.5	5.9
	10	7.7	8	6.7	5.5
	100	7.8	8.2	6.5	5.7
	1000	8.2s	8.8	6.7s	(6.3)
	10000	7.8	7.8	6.5	5.8
140	1	7.4s	8.5	5.8	5.7
	10	8.5s	8.7	7	6.4
	100	8.4	8.4	6.6	5.8
	1000	7.6s	8.5	5.5s	(5.4)
	10000	7s	8.5	5.6	5.6
160	1	8.1s	9.4	7.2	6.7
	10	7.8s	8.2	6.2s	(5.9)
	100	9.1	8.8s	6.9	6.4
	1000	9.2	9	7	6.3
	10000	8.1	7.7	6.5	5.5
180	1	6.6s	8.5	5.5	5.2
	10	7.9	8.9	6	5.6
	100	7.7	8.3	6.3	5.3
	1000	7.6	7.8	6.5	5.5
	10000	8.2	7s	8.1	5.2

B9 X-ray peak intensities for aged 8350

Sample	Aging °C	hours	E, MPa	Elongation, %
8350 Q		0	584	302
8350 Q	AW 100	24	527	249
8350 Q	A 160	24	597	155
8358 Q		0	265	>460
8358 Q	AW 100	24	300	360
8358 Q	A 160	24	377	>460
Z.91 AHS Q		0	198	>460
Z.91 AHS Q	AW 100	24	379	>460
Z.91 AHS	A 160	24	202	>460
Z. 726 Q		0	128	359
Z. 726 Q	AW 100	24	170	370
Z. 726 Q	A 160	24	160	127

Q - quenched from melt to ice water
AW - annealed in boiling water
A- annealed in air

B10 Tensile properties of tubing materials as-quenched and after aging

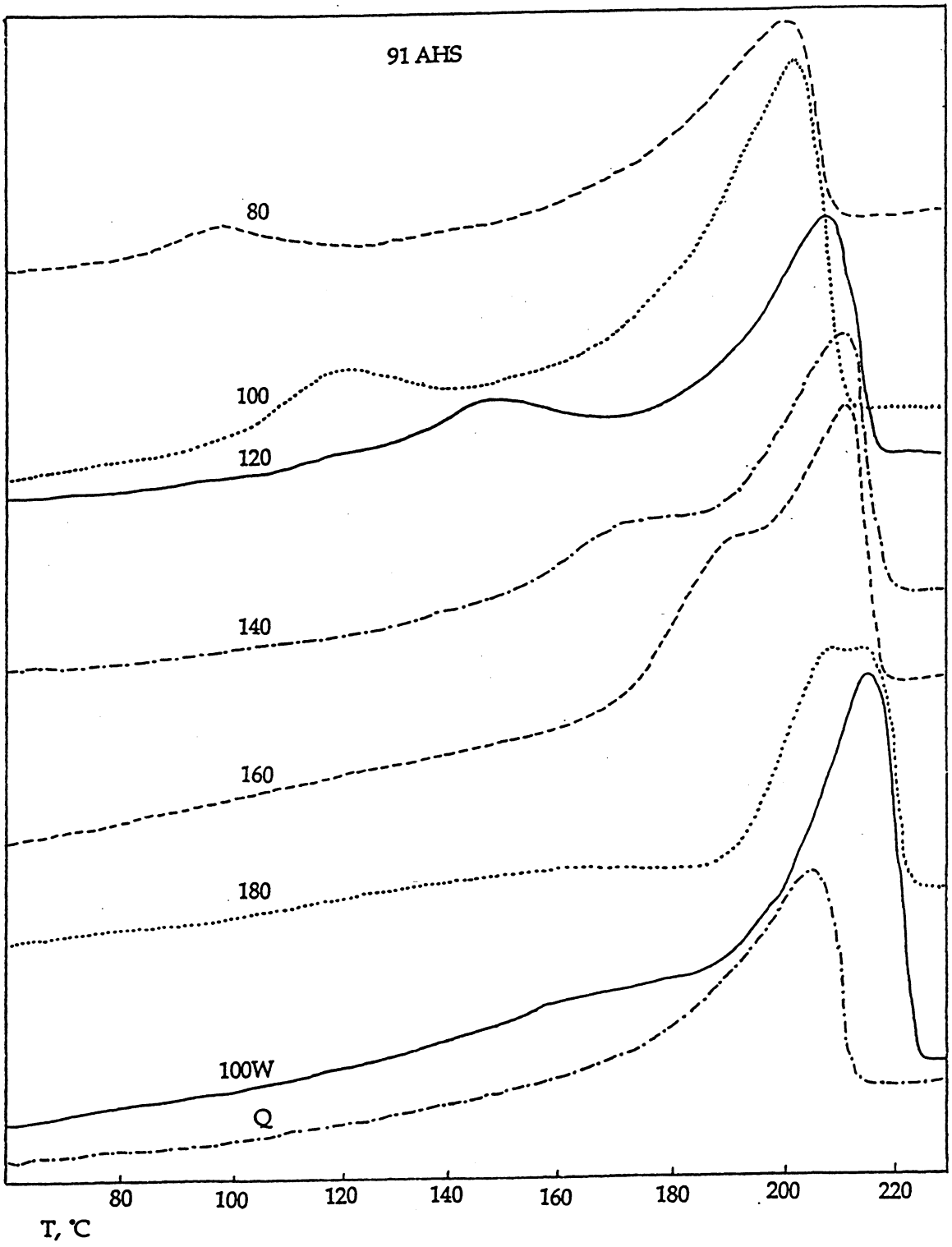

B1. DSC melting peaks of the sample 91AHS as-quenched (Q) and annealed 10000 min. at various temperatures. Scan rate 20°C/min.

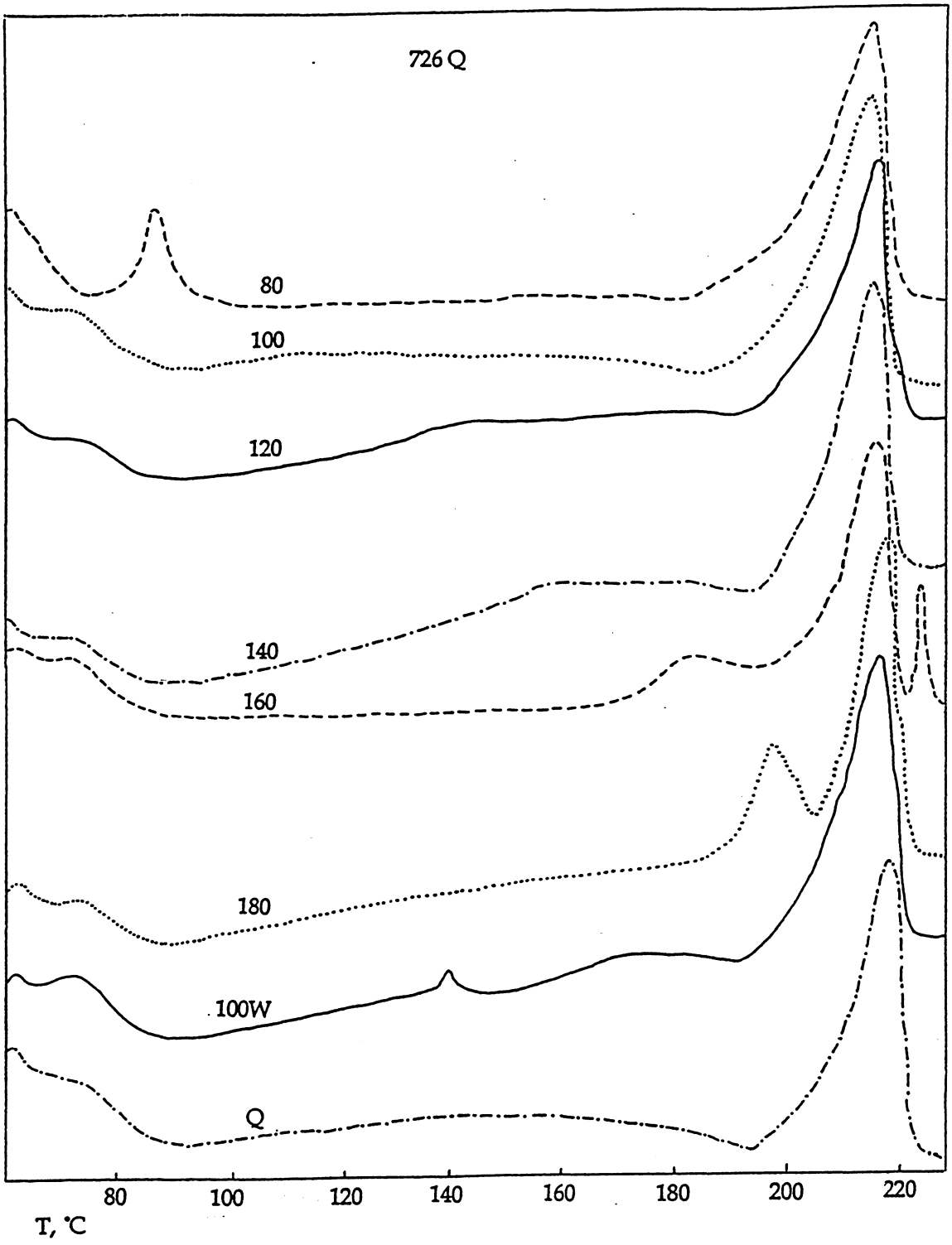

B2. DSC melting peaks of the sample 726 as-quenched and annealed 10000 min. at various temperatures. Scan rate 20°C/min.

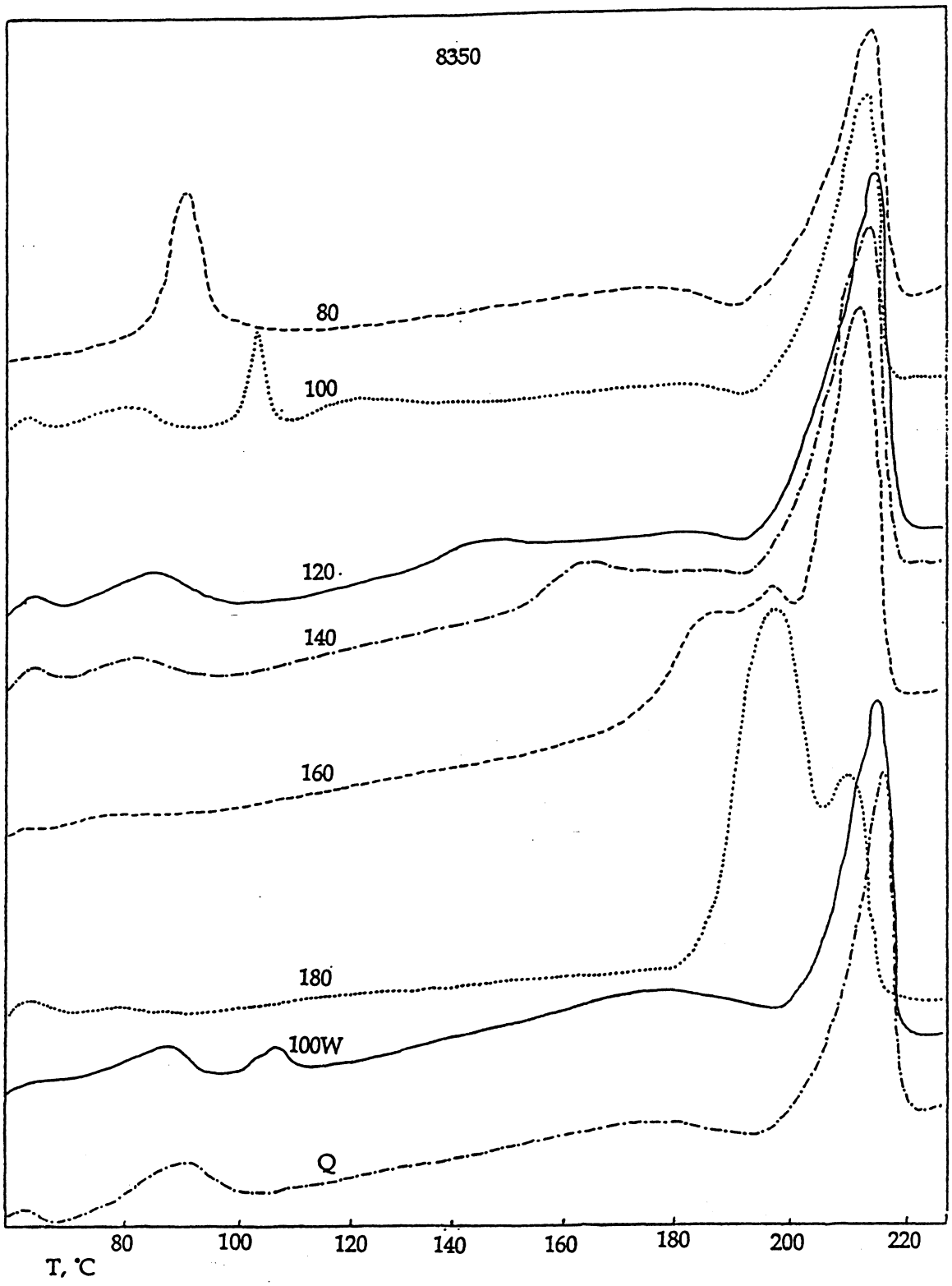

B3. DSC melting peaks of the sample 8350 as-quenched and annealed 10000 min. at various temperatures. Scan rate 20°C/min.

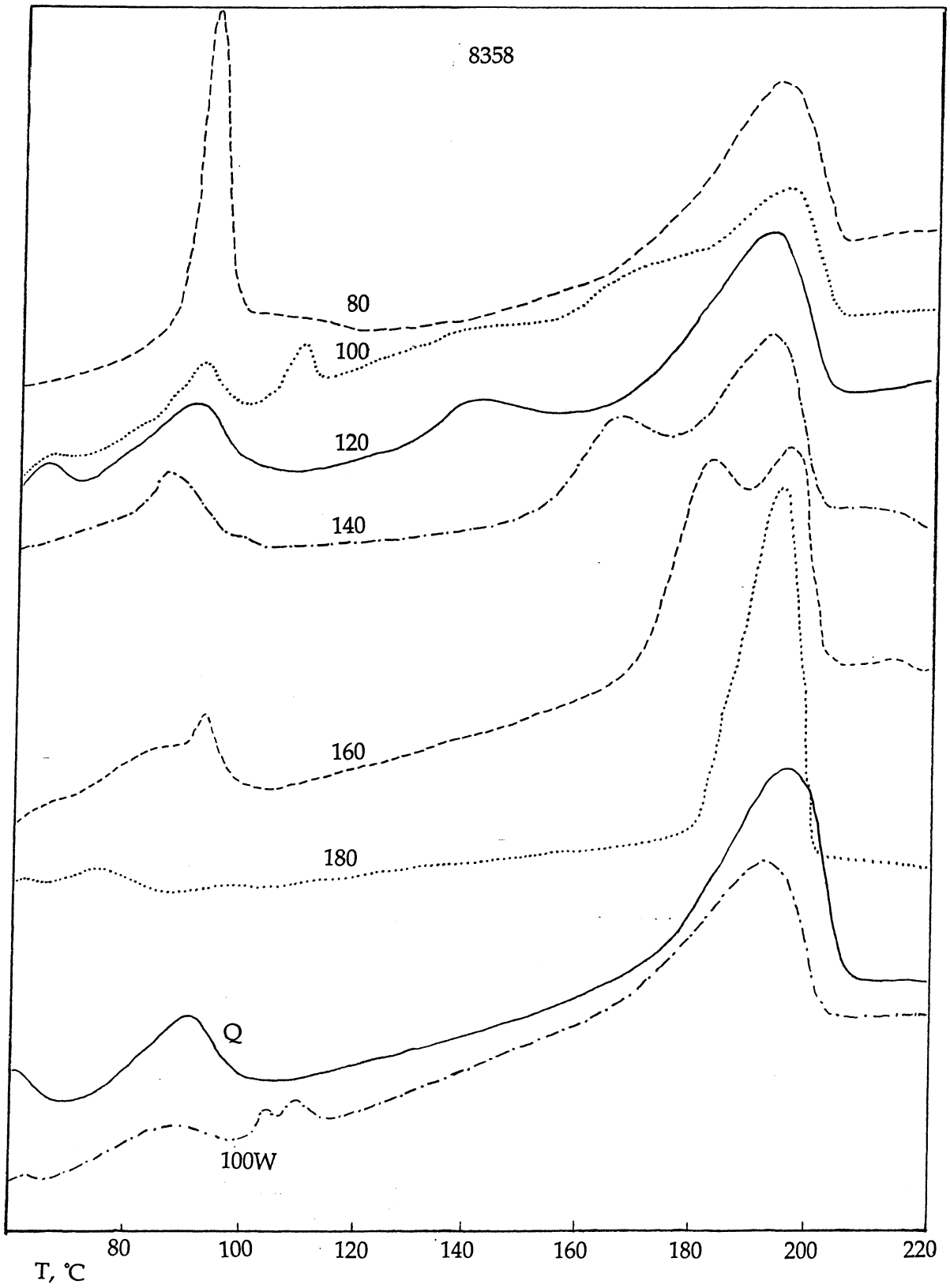

B4. DSC melting peaks of the sample 8358 as-quenched and annealed 10000 min. at various temperatures. Scan rate 20°C/min.

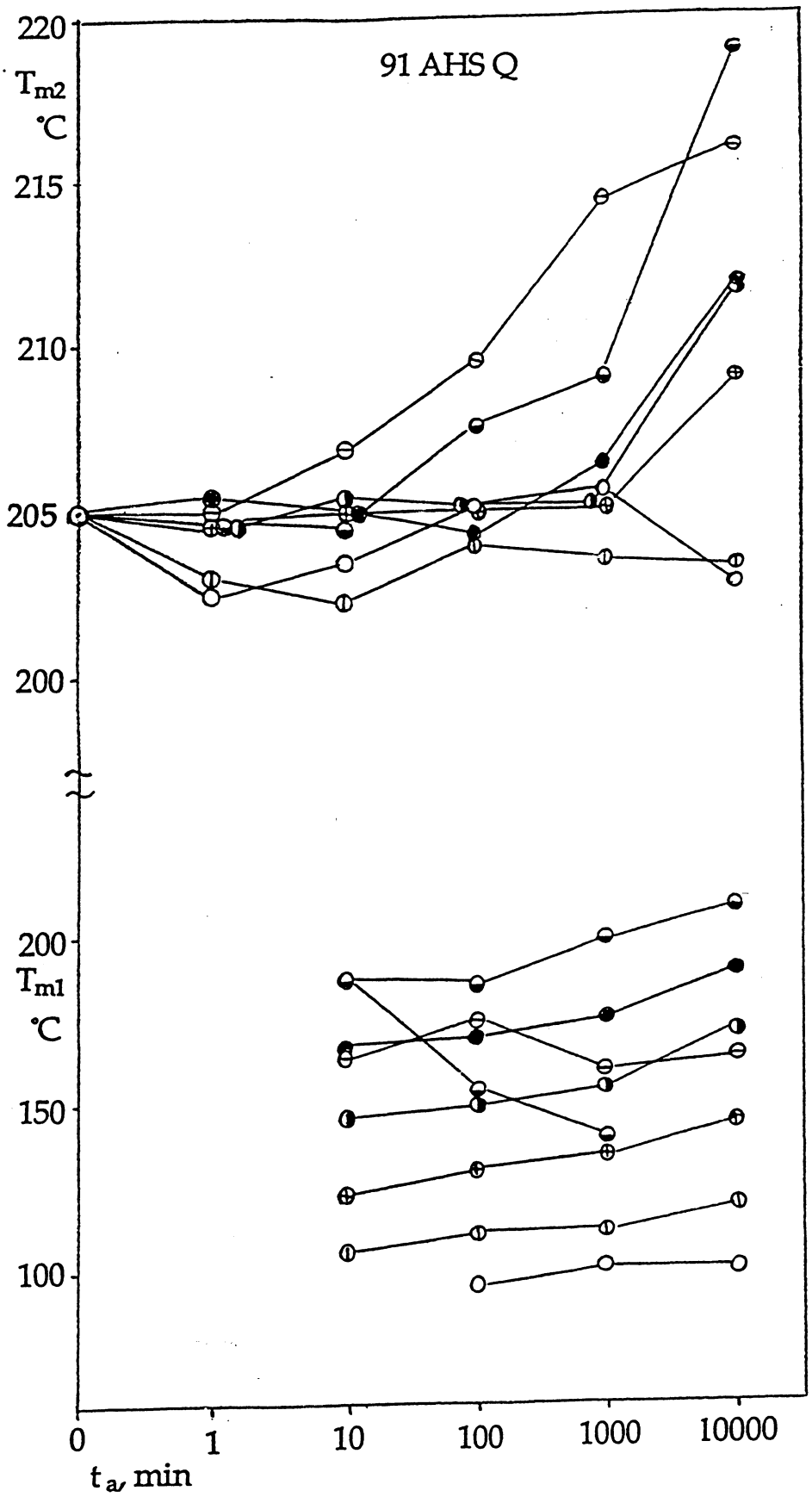

B5. Melting temperatures T_{m2} and T_{m1} values of the sample 91AHS annealed at various temperatures as a function of annealing time t_a. The annealing temperatures T_a are marked: 80°C O, 100°C ◐, 100°W ⊖, 120°C ⊕, 140°C ◑, 160°C ● and 180°C ◒. These symbols also apply for all subsequent figures.

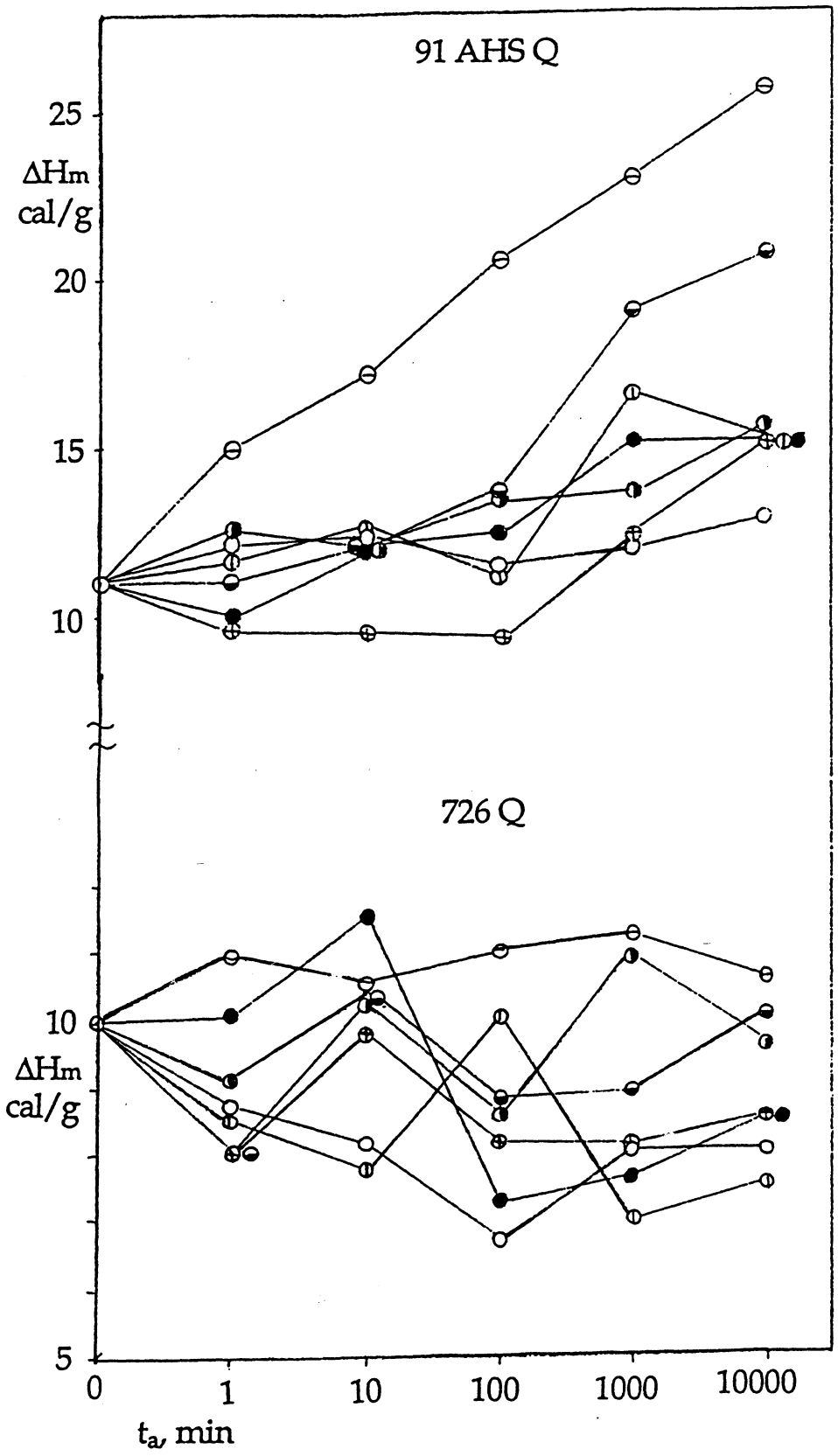

B6. Heats of melting of PA peaks of the sample 91AHS Q and 726 Q as function of T_a and t_a.

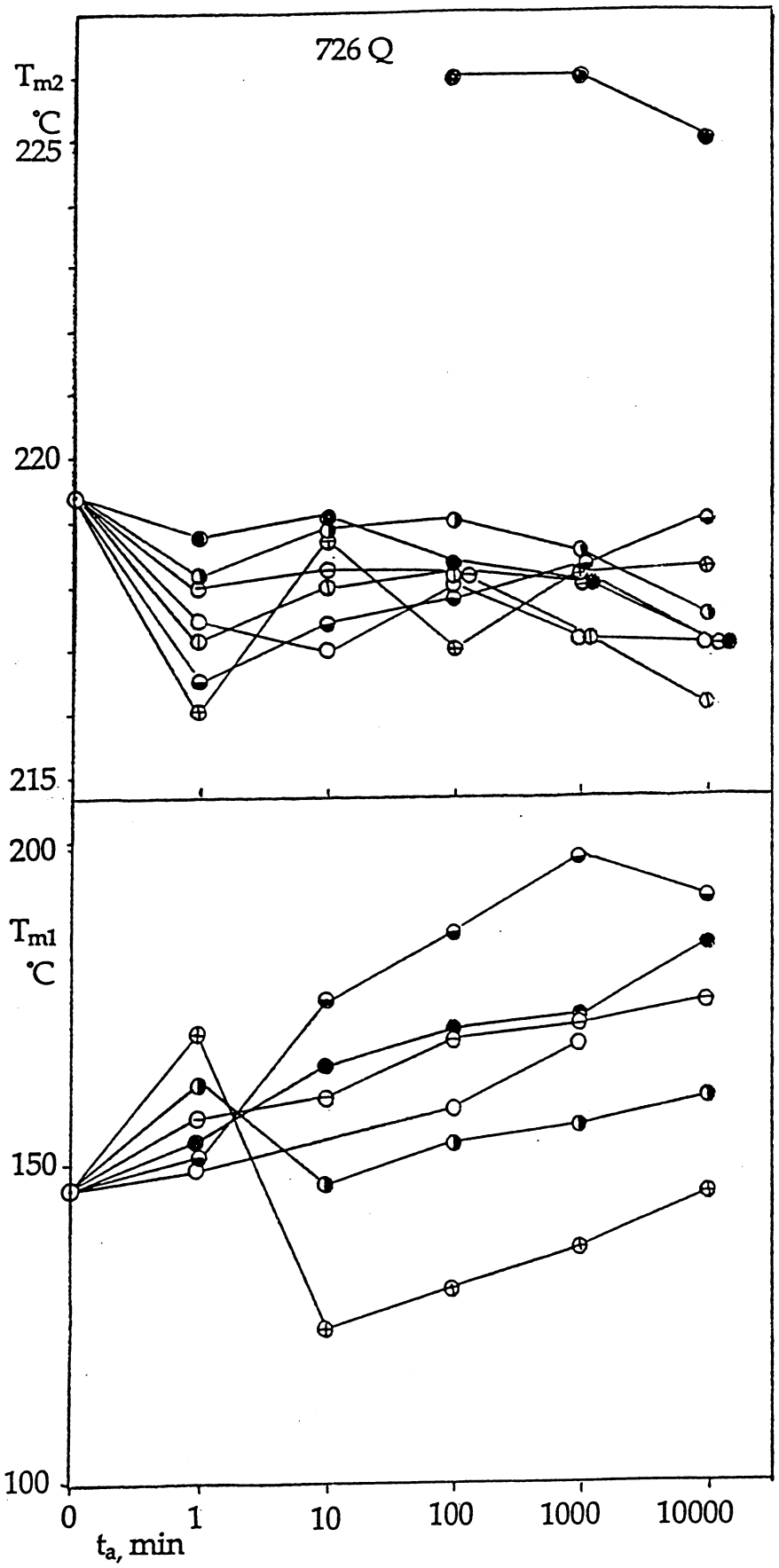

B7. Melting temperature T_{m2} and T_{m1} values of the sample Zytel 726 Q annealed at various T_a and t_a. The drop in T_{m1} for the 120 and 140° curves corresponds to the development of the annealing peak.

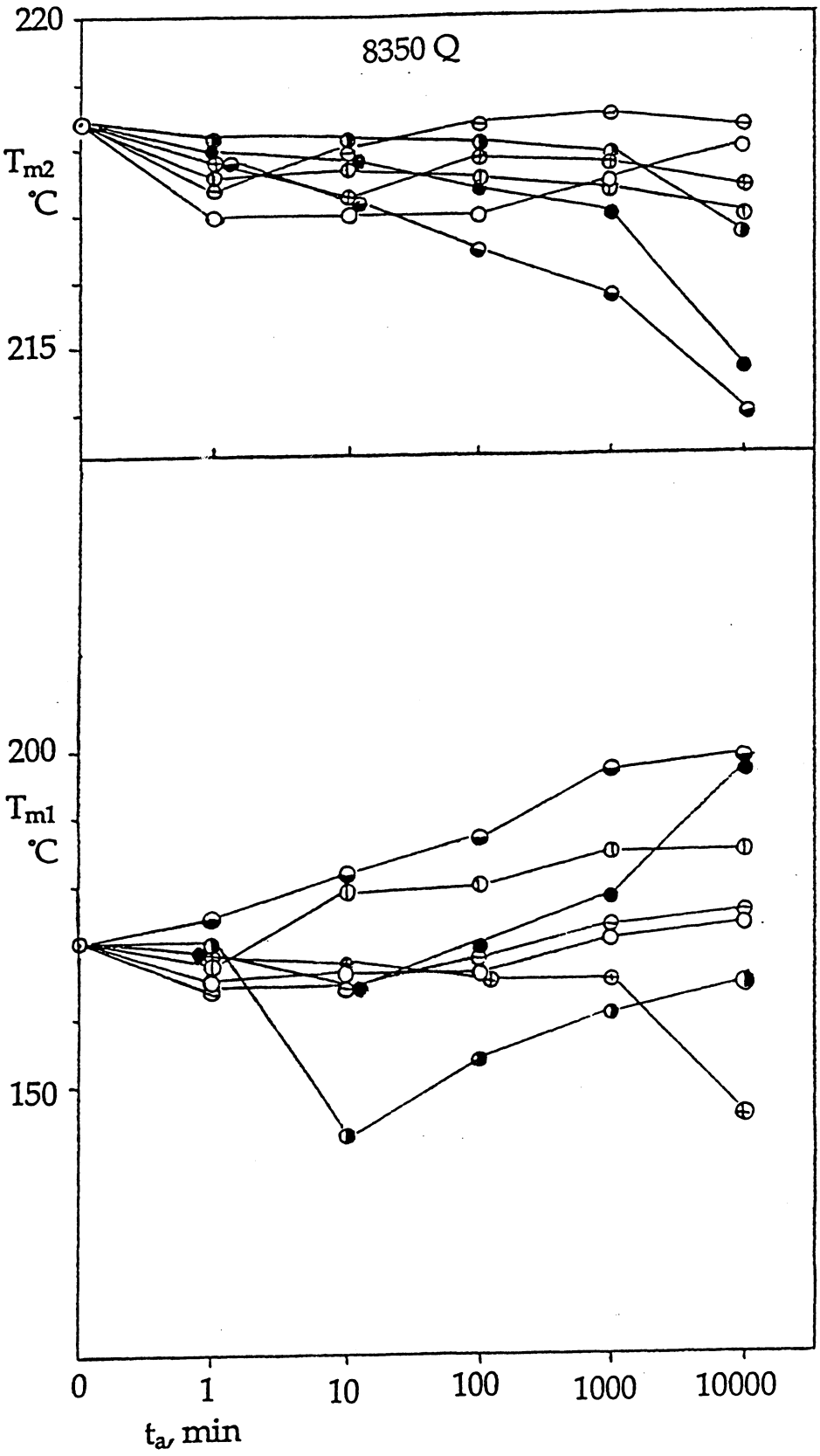

B8. Melting temperature T_{m2} and T_{m1} values of the sample 8350 Q annealed at various T_a and t_a.

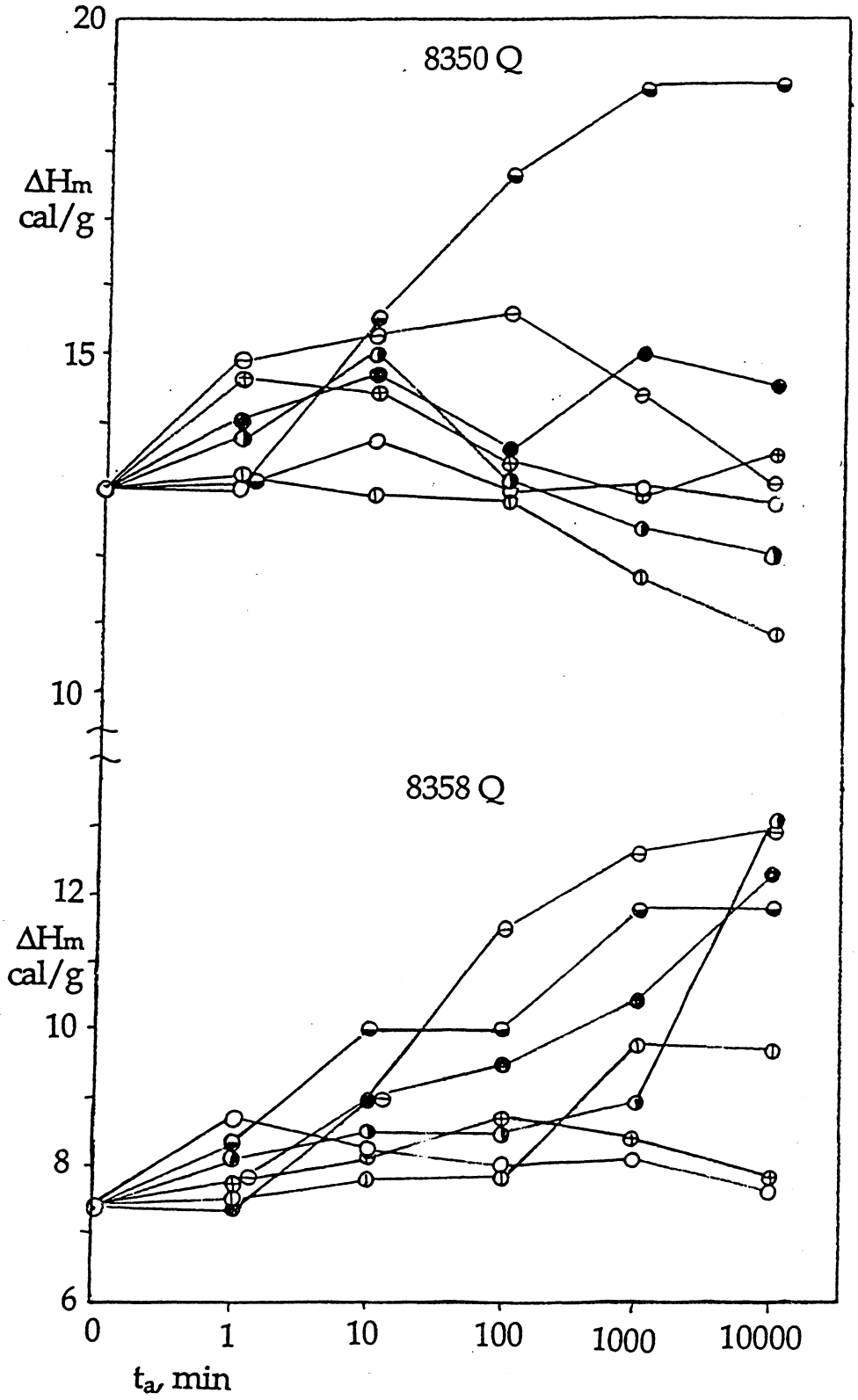

B9. Heats of melting of PA peaks for the sample 8350 Q and 8358 Q as a function of T_a and t_a.

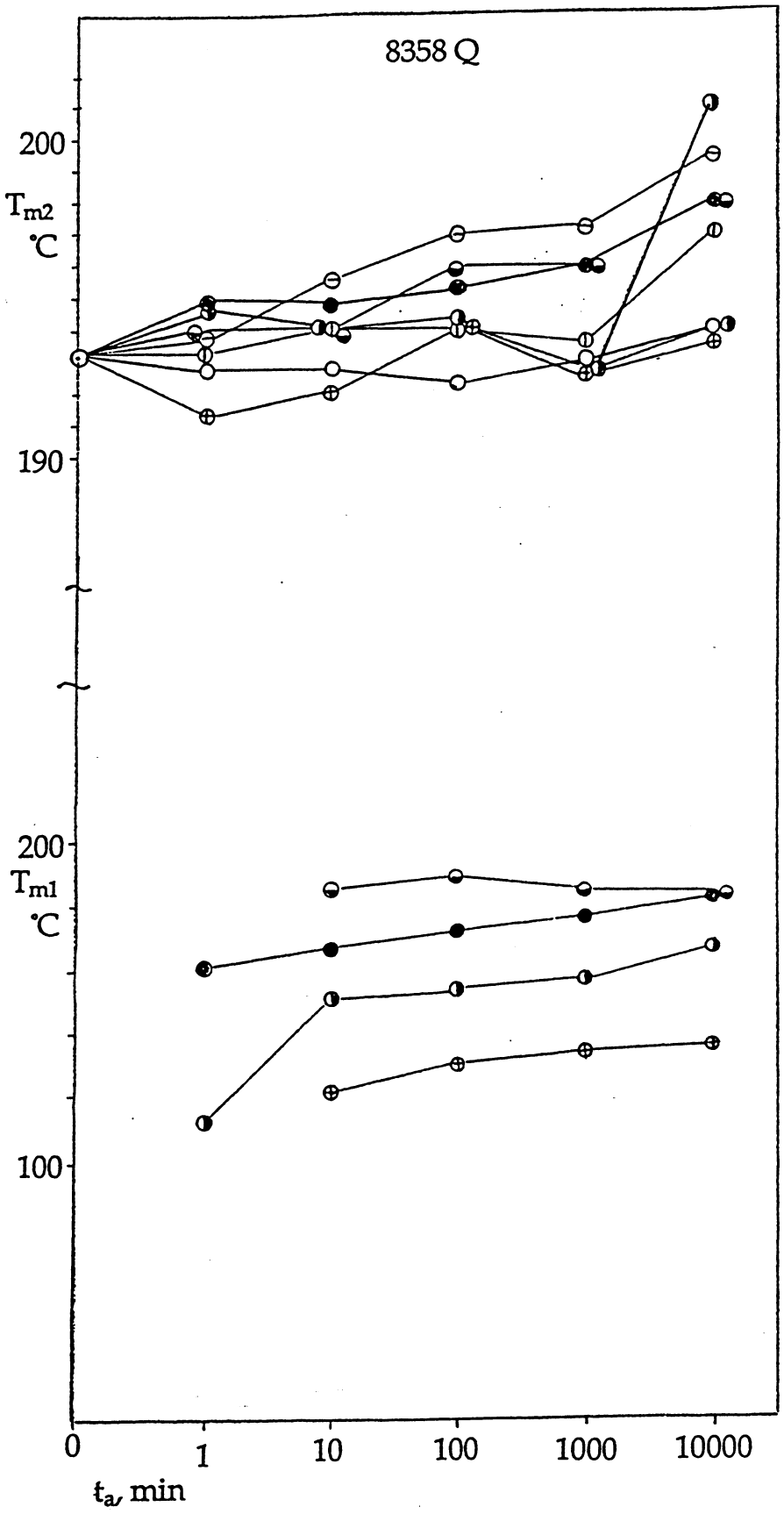

B10. Melting temperature T_{m2} and T_{m1} values of the sample 8358 Q annealed at various T_a and t_a.

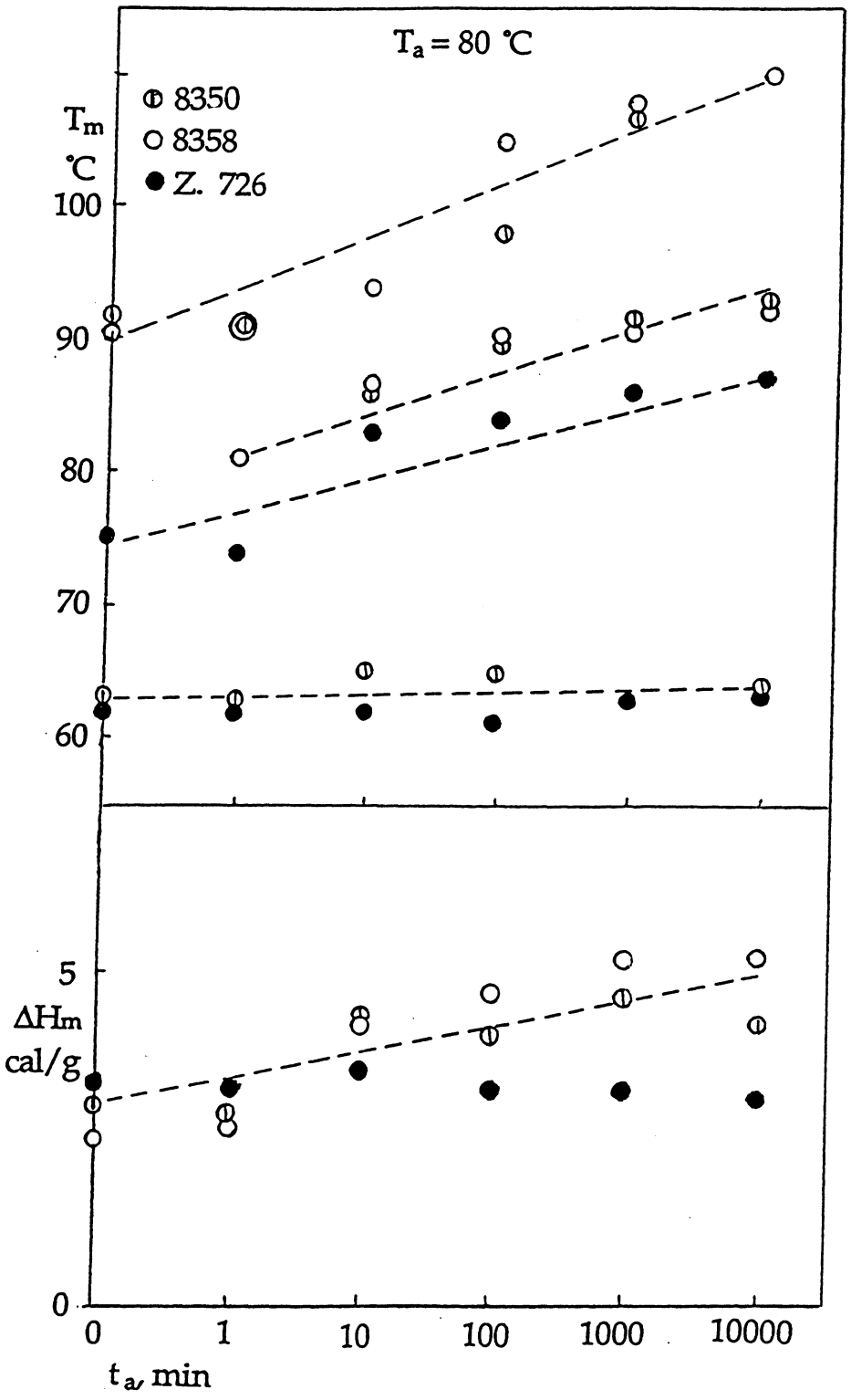

B11. Melting peaks of the polyetheylene crystalline sequences of the polyolefine-copolymer of samples 8350, 8358 and 726 annealed at 80°C for various t_a.

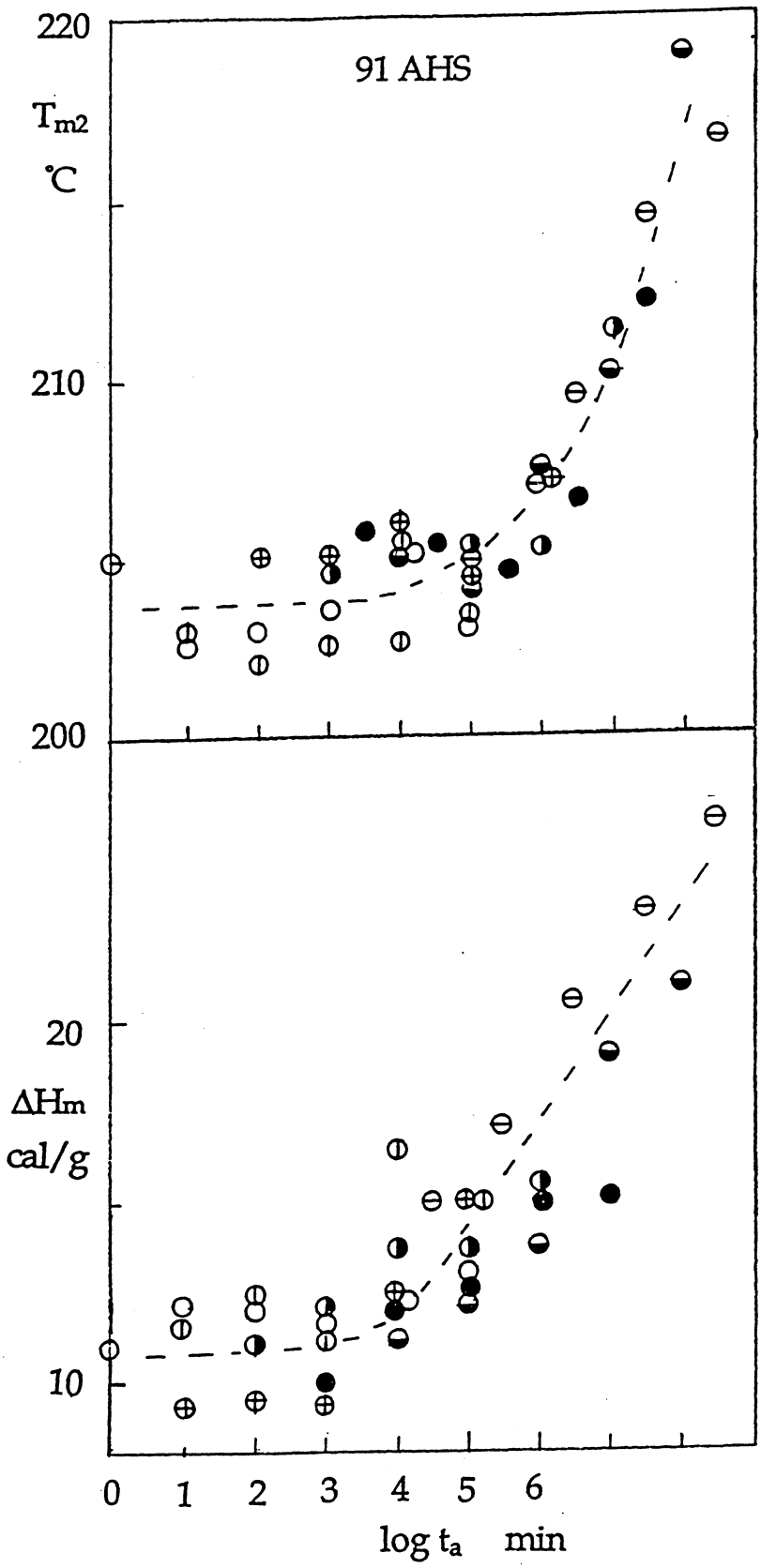

B12. Time-temperature superposition for aging sample 91AHS T_{m2} and ΔH_m values.

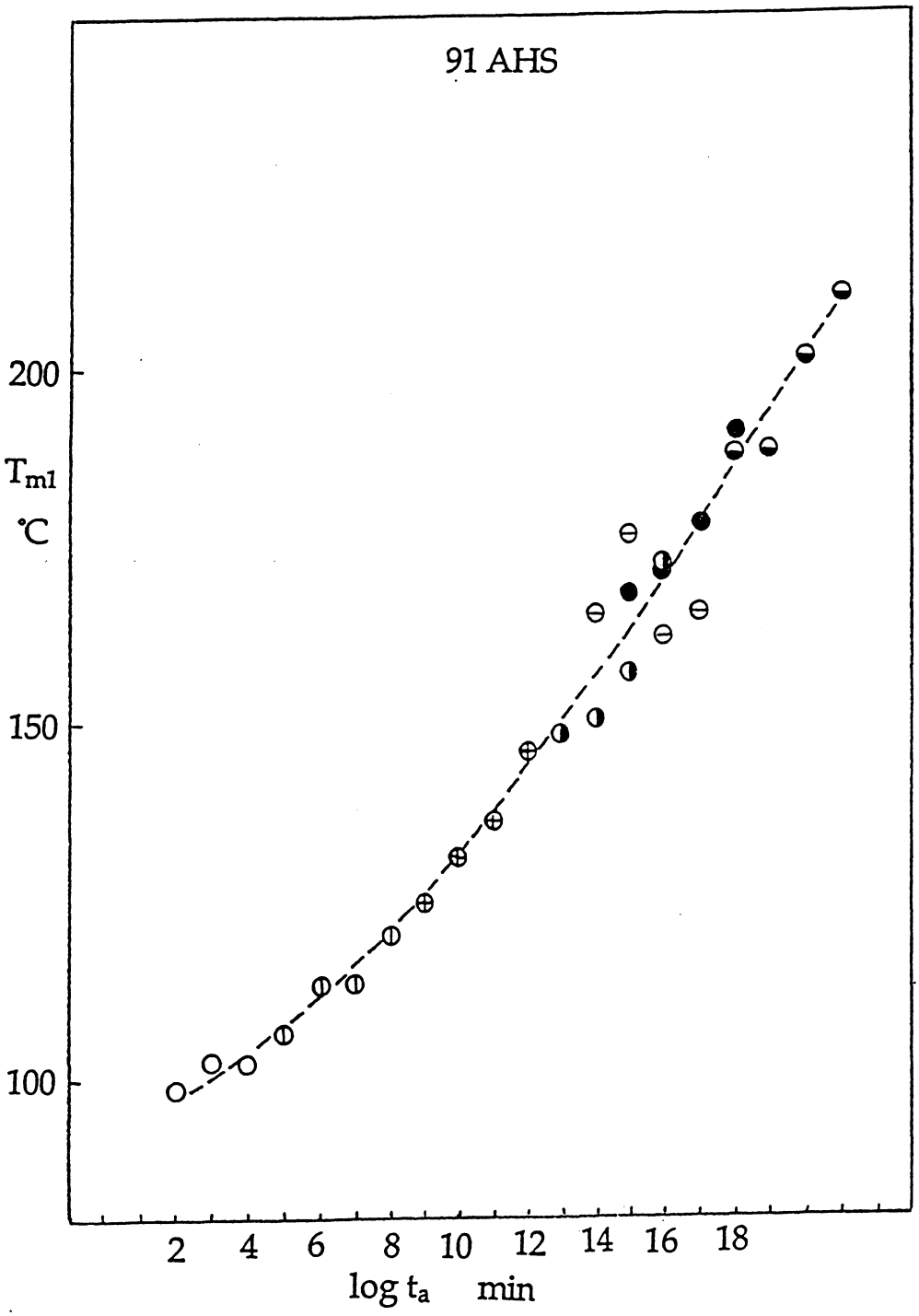

B13. Time-temperature superposition for aging sample 91AHS;T_{m1} values.

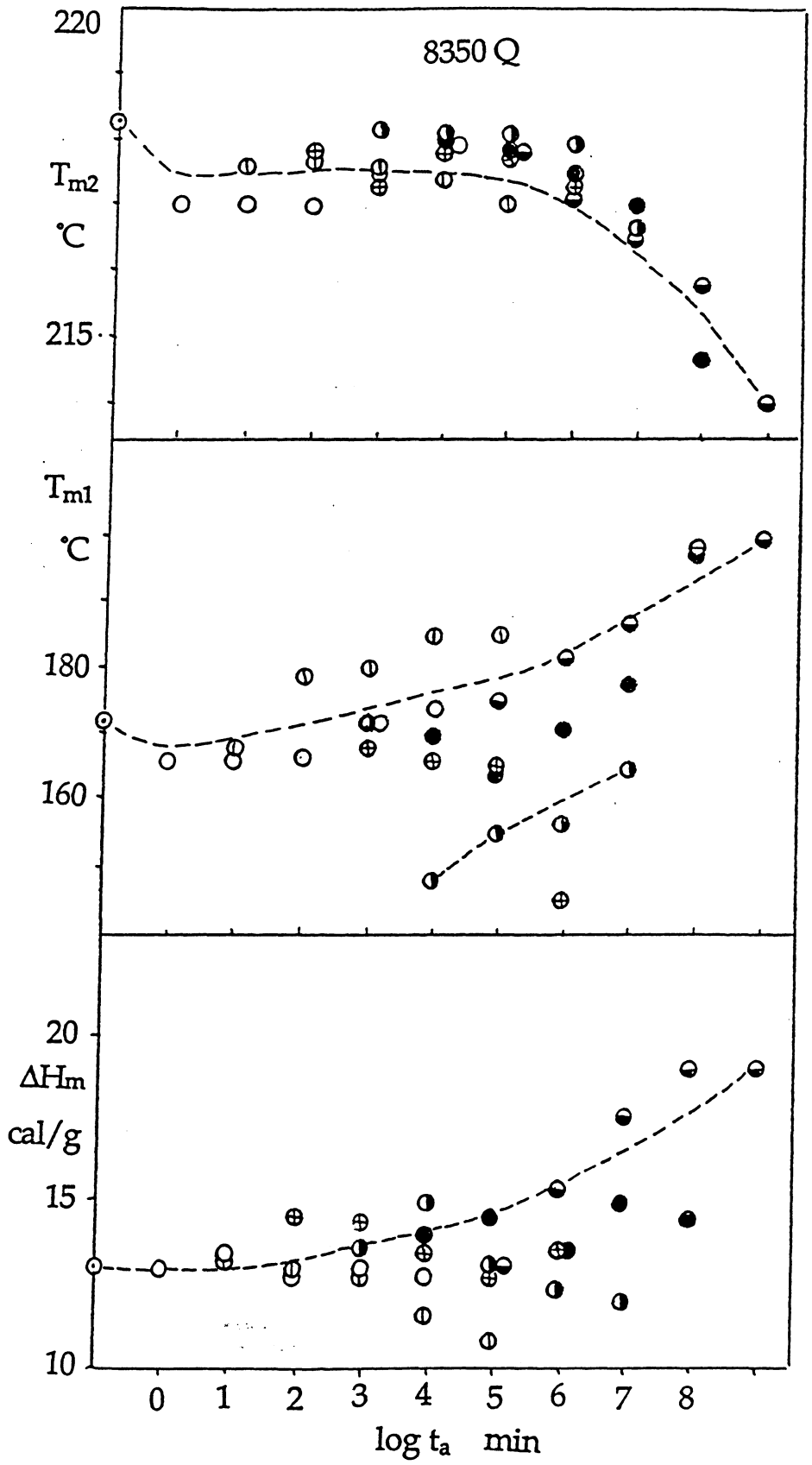

B14. Time-temperature superposition for aging sample 8350.

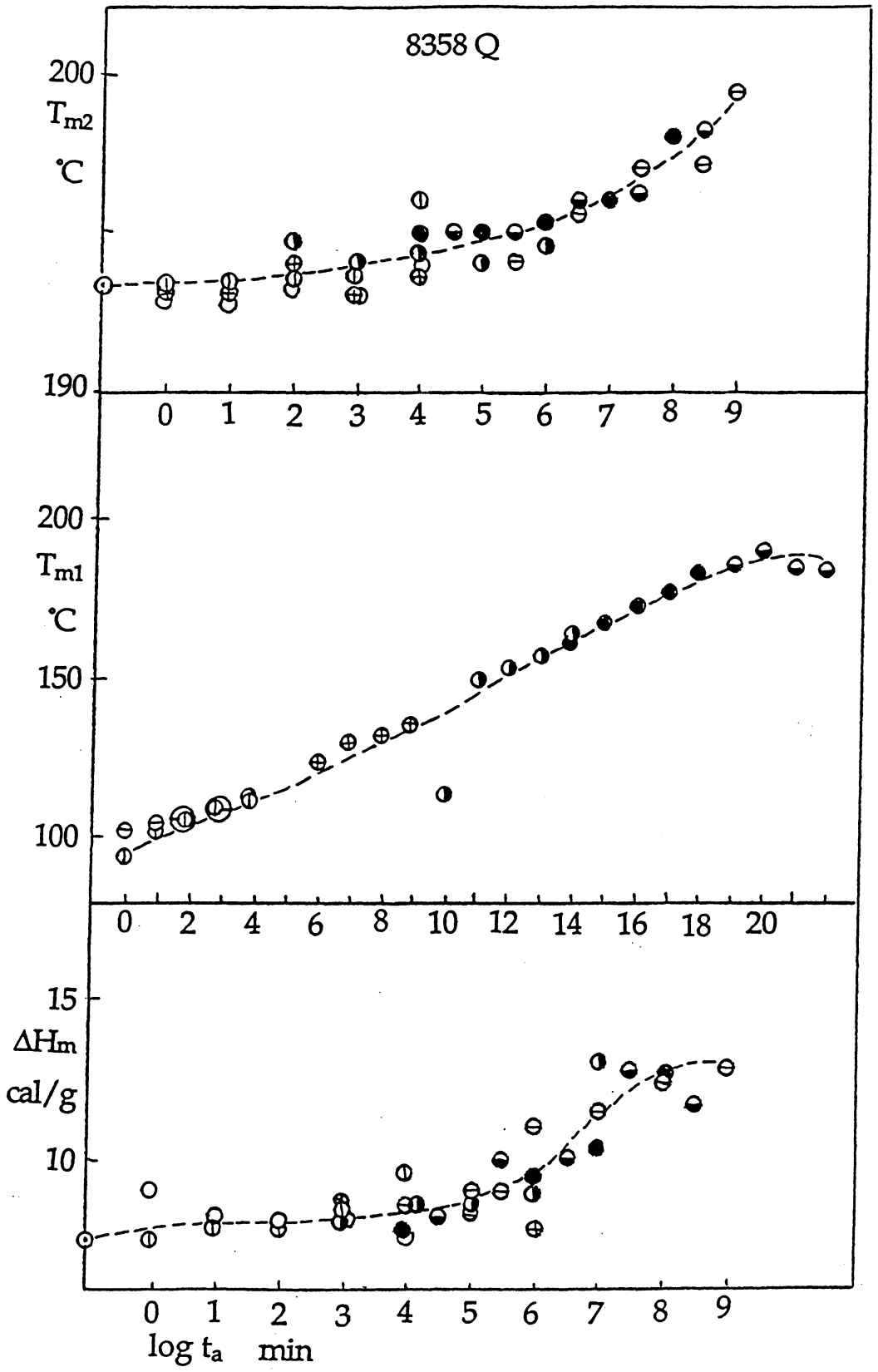

B15. Time-temperature superposition for aging sample 8358.

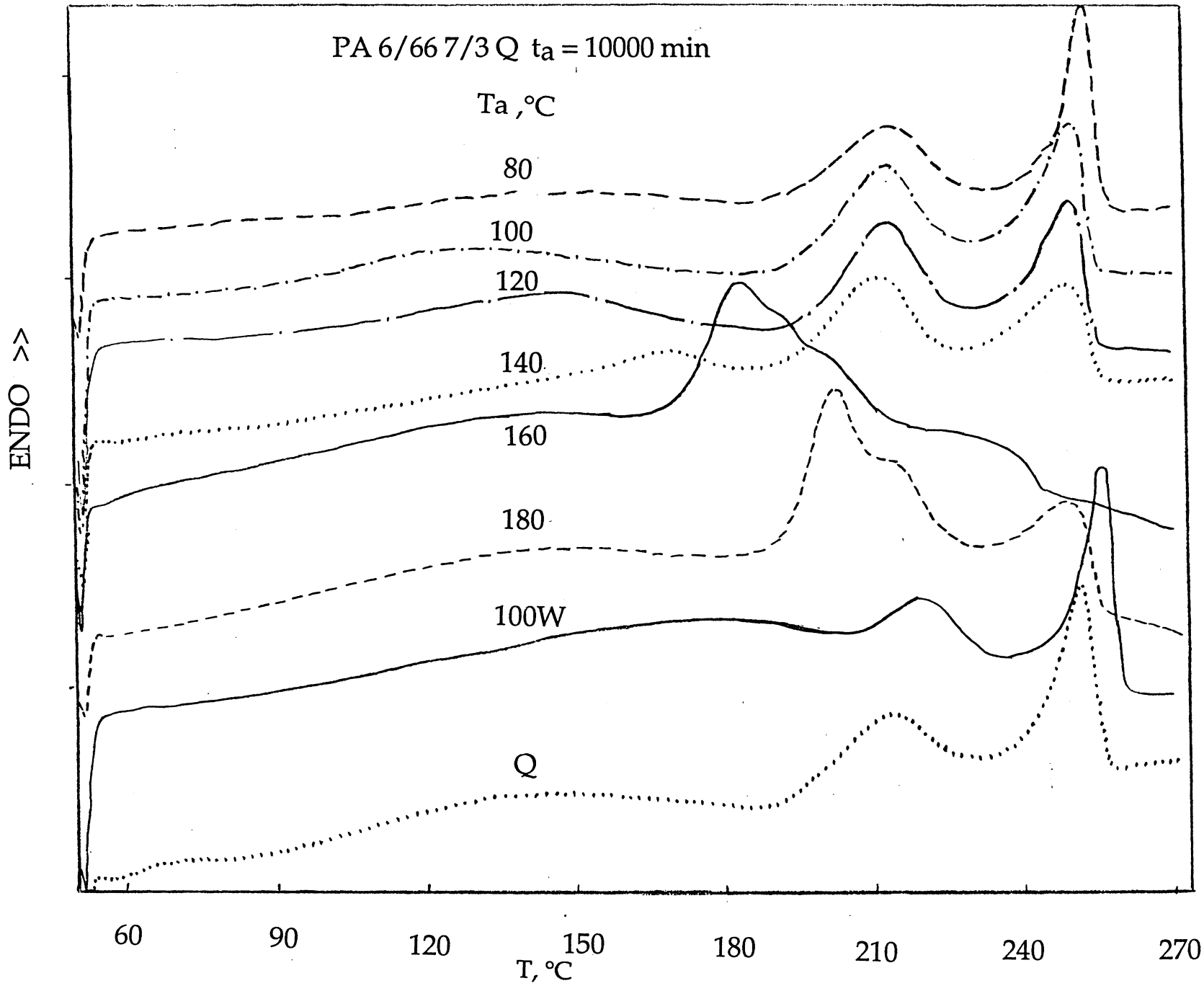

B16. DSC melting peaks of a PA6/66 7/3 blend as-quenched and annealed 100000 min at various temperatures. Scan rate 20°C/min.

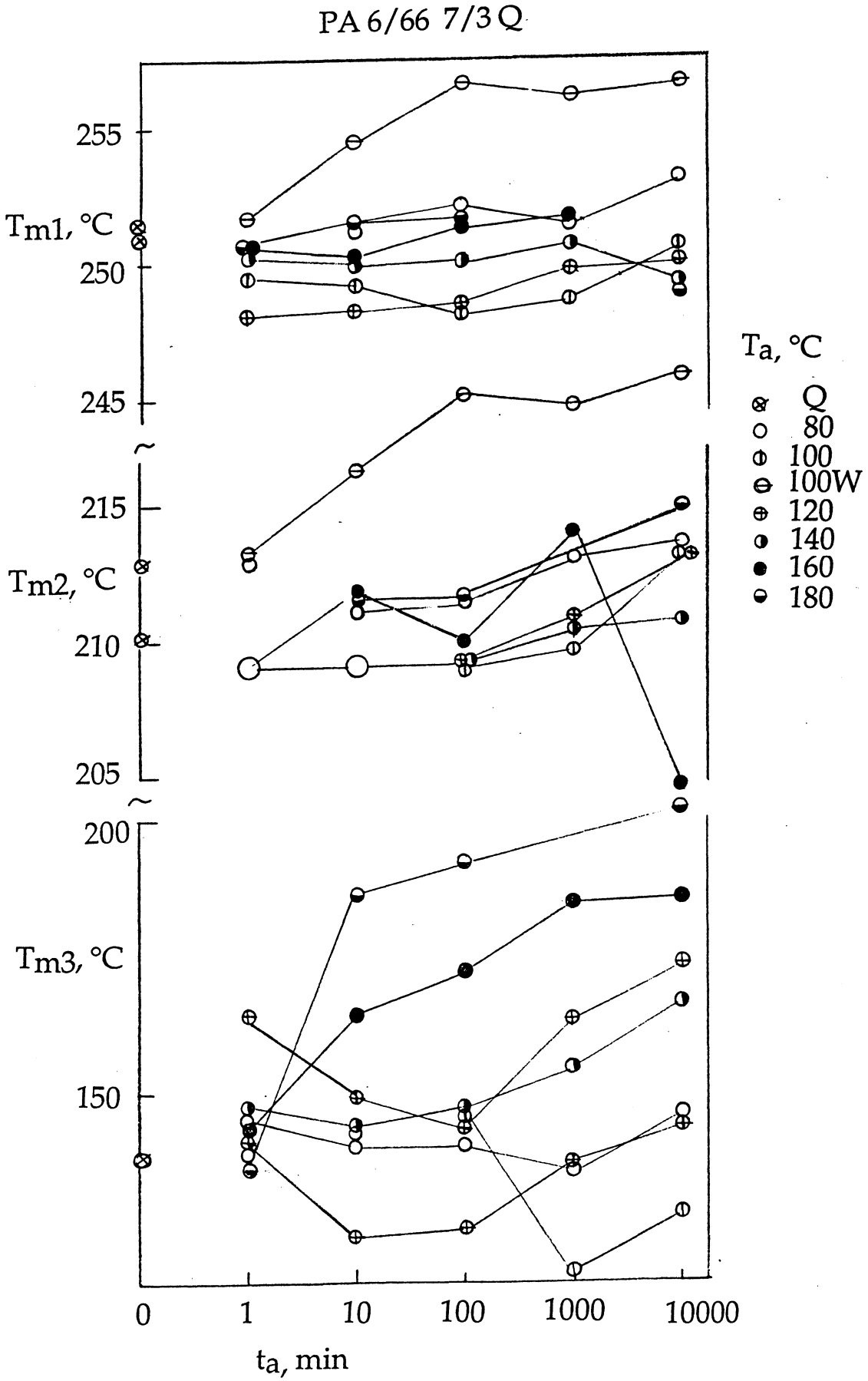

B17. Melting temperatures of the PA6/66 7/3 blend annealed at various T_a and t_a. T_{m3} in the annealing peak (T_m(a)).

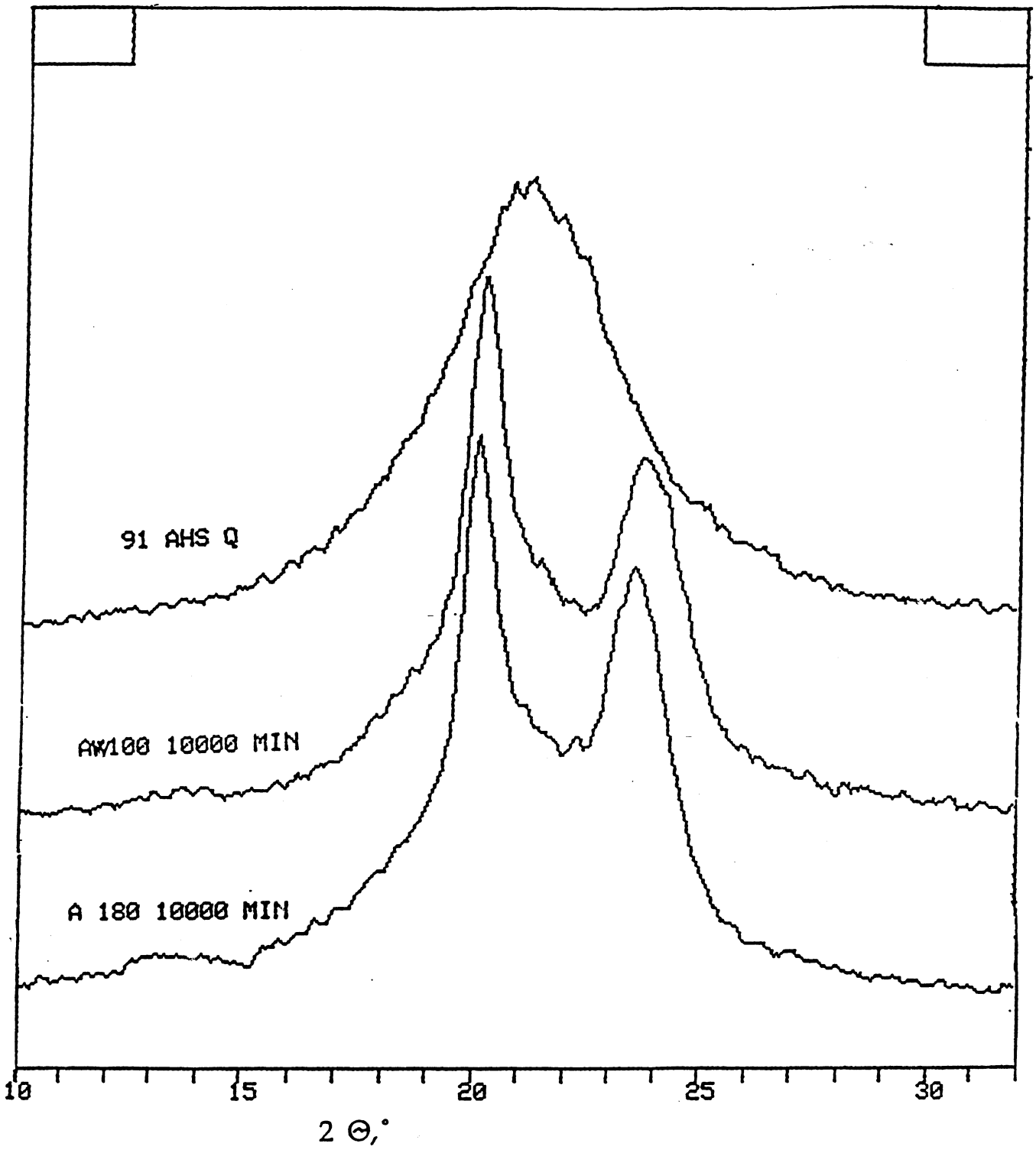

B18. X-ray diffraction patterns of 91AHS samples, quenched, annealed 10000 min. in boiling water or at 180°C in air.

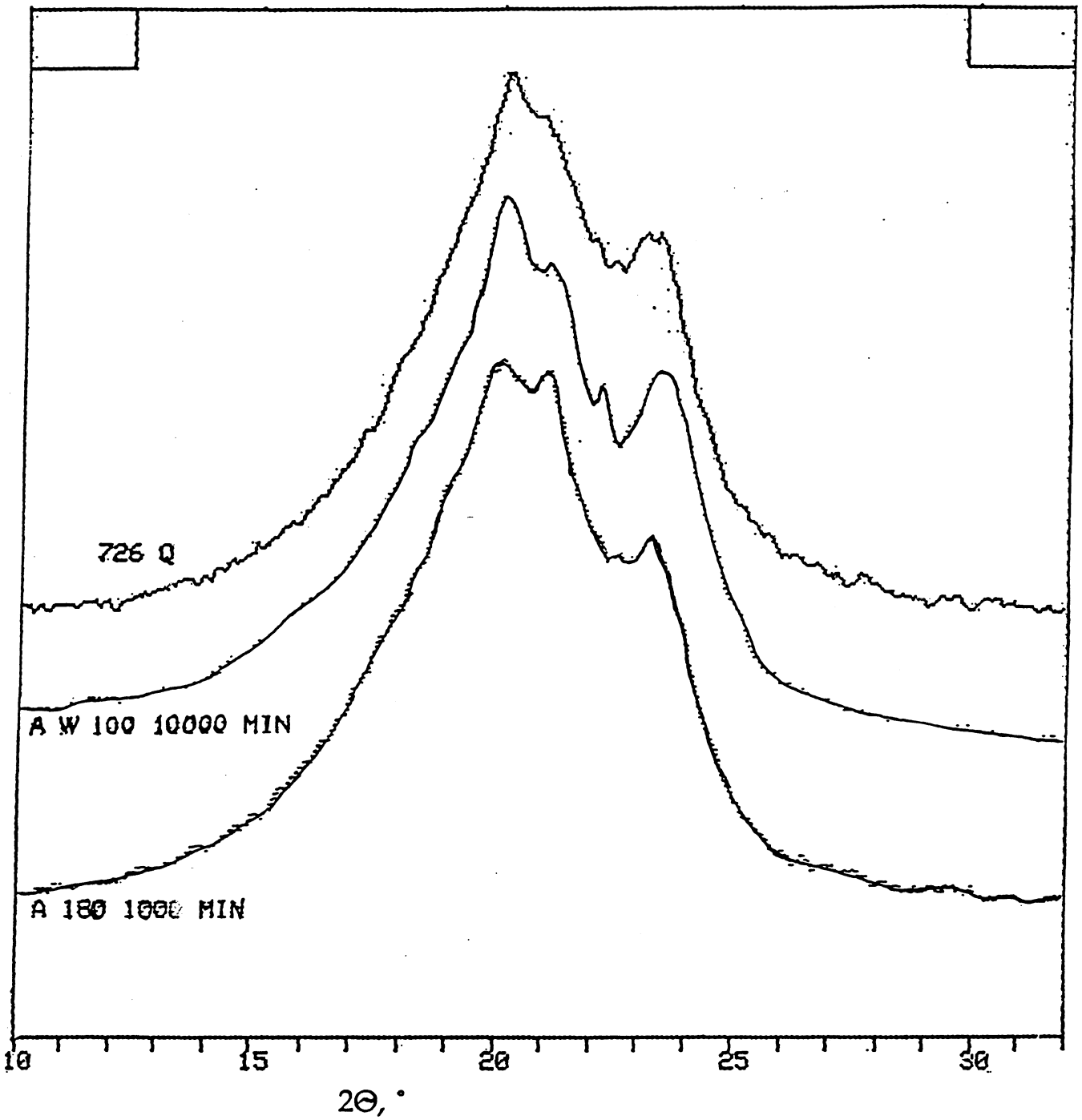

B19. X-ray diffraction patterns of 726 samples, quenched, annealed 10000 min. in boiling water and at 180°C in air.

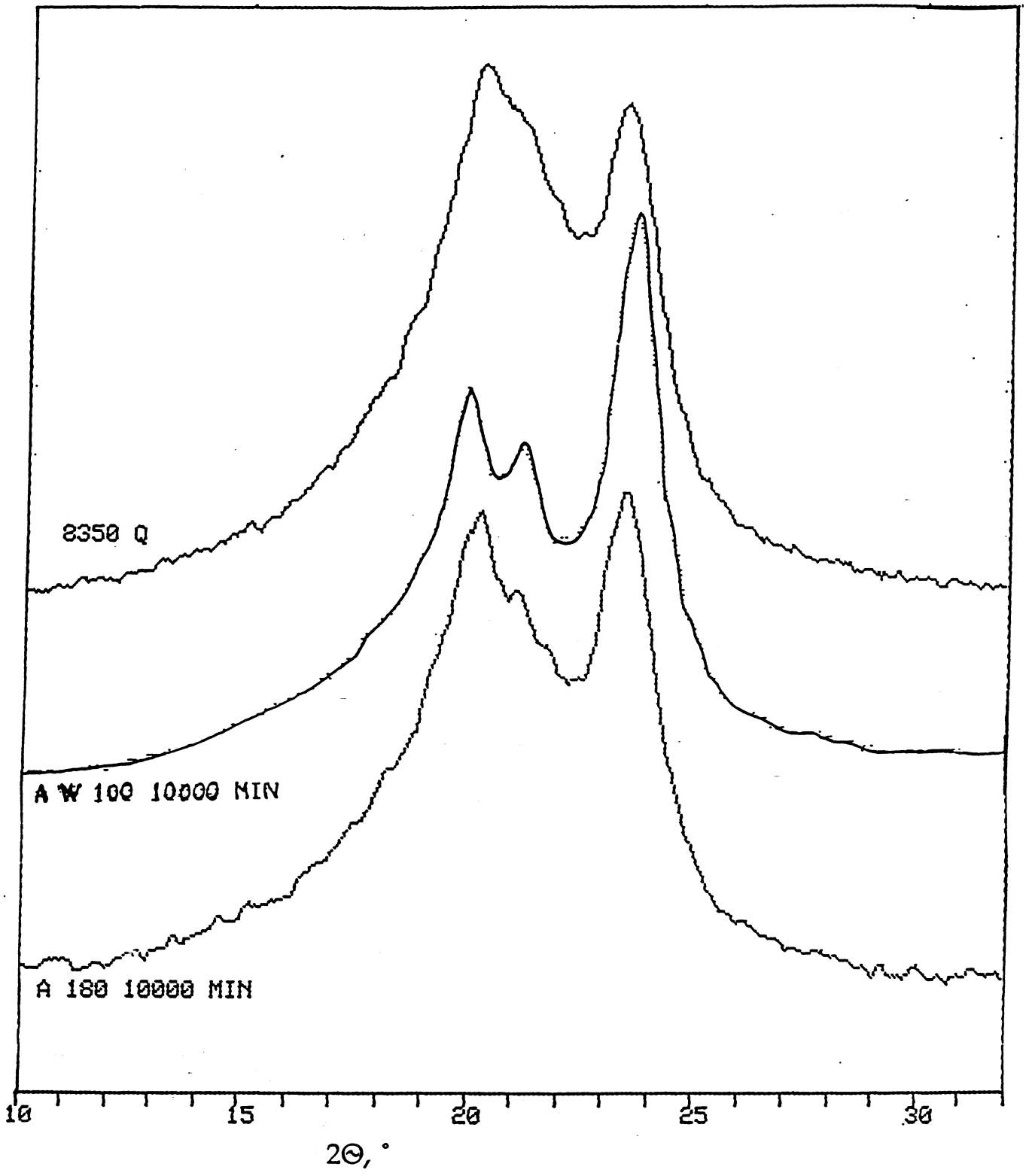

B20. X-ray diffraction patterns of 8350 samples, quenched, annealed 10000 min. in boiling water and at 180°C in air.

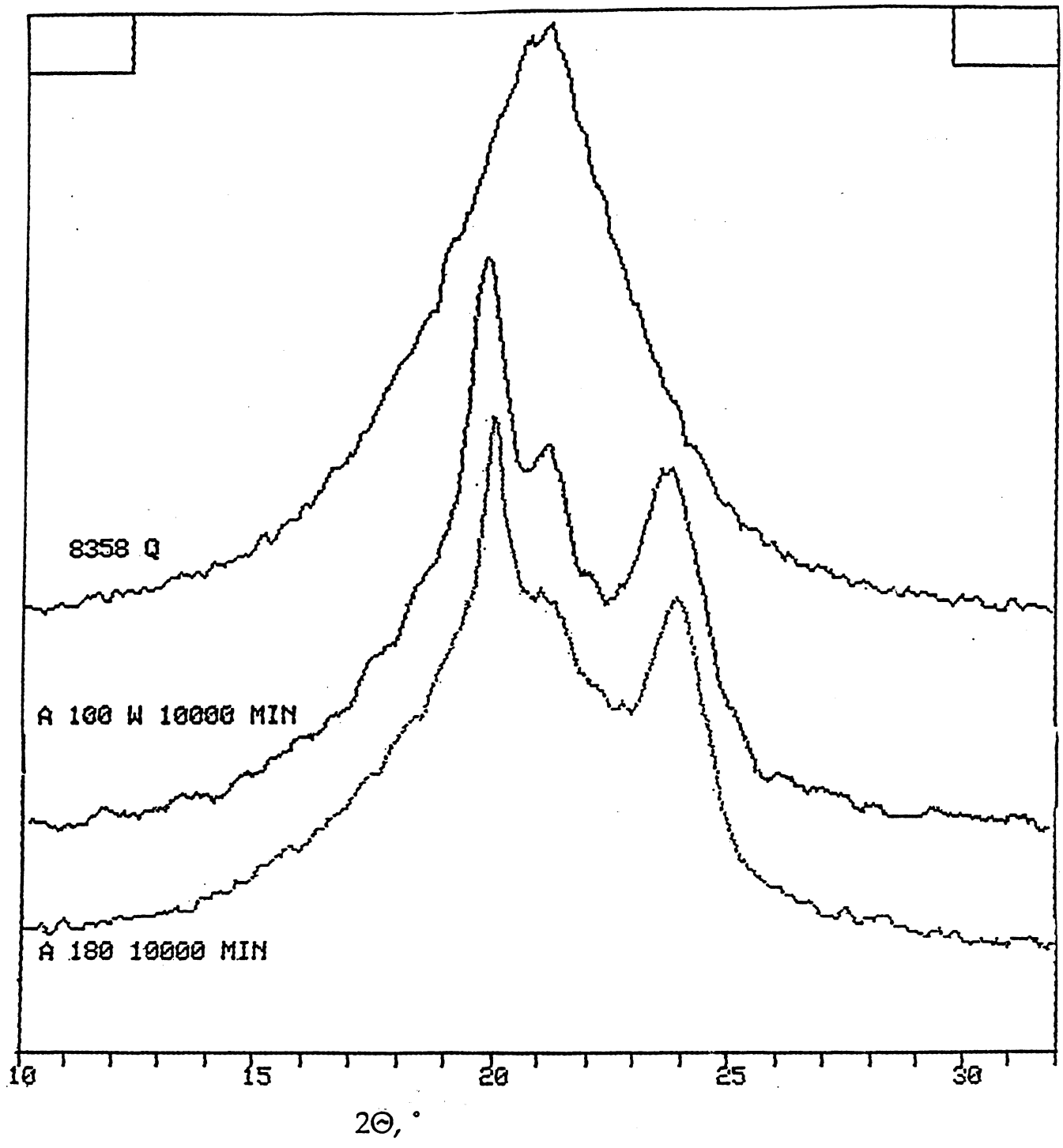

B21. X-ray diffraction patterns of 8358 samples, quenched, annealed 10000 min. in boiling water and at 180°C in air.

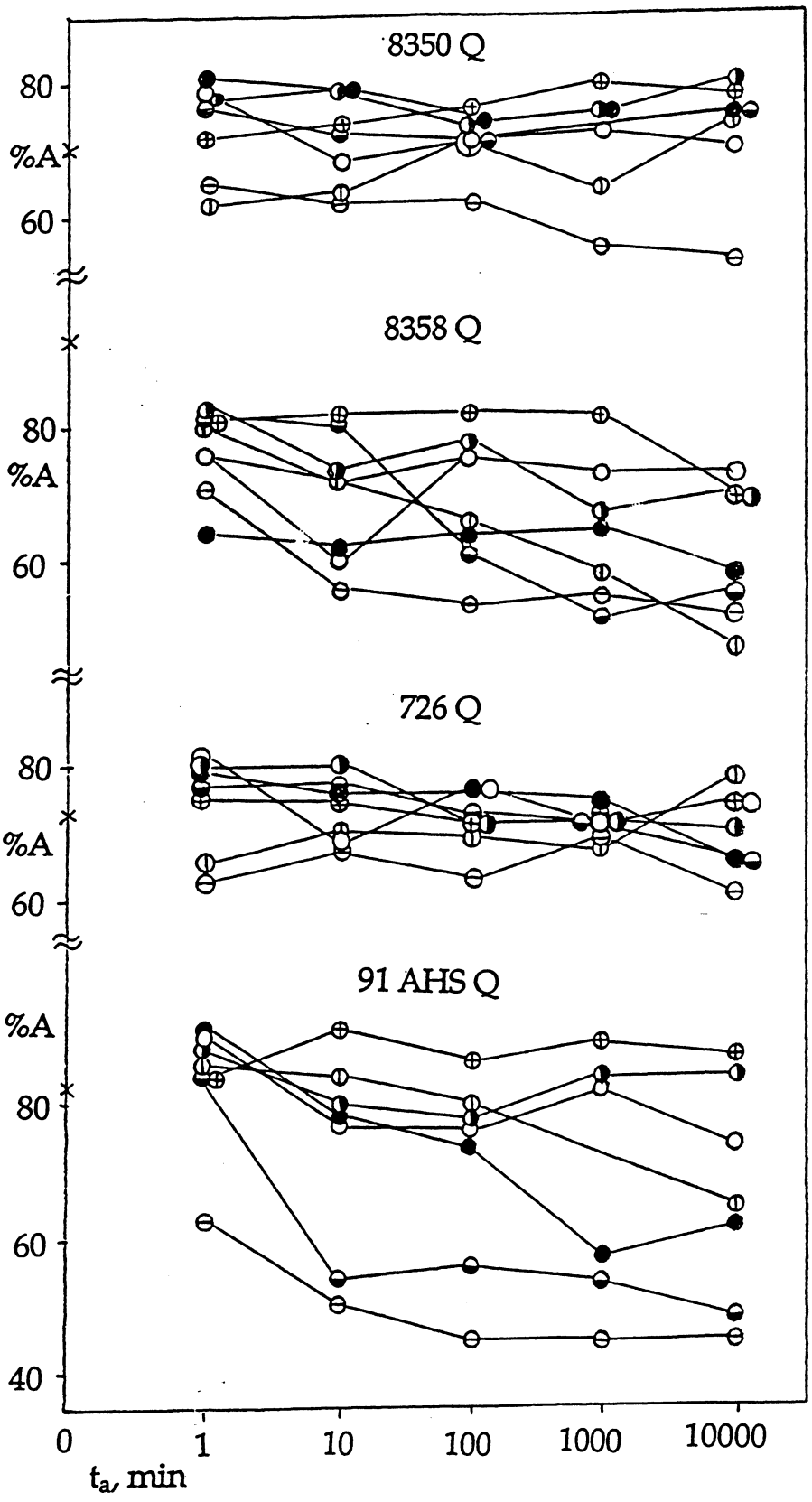

B22. The changes of the amorphous phase index, %A, as a function of aging temperature and time for samples 8350 Q, 8358 Q, 726 Q and 91AHS Q.

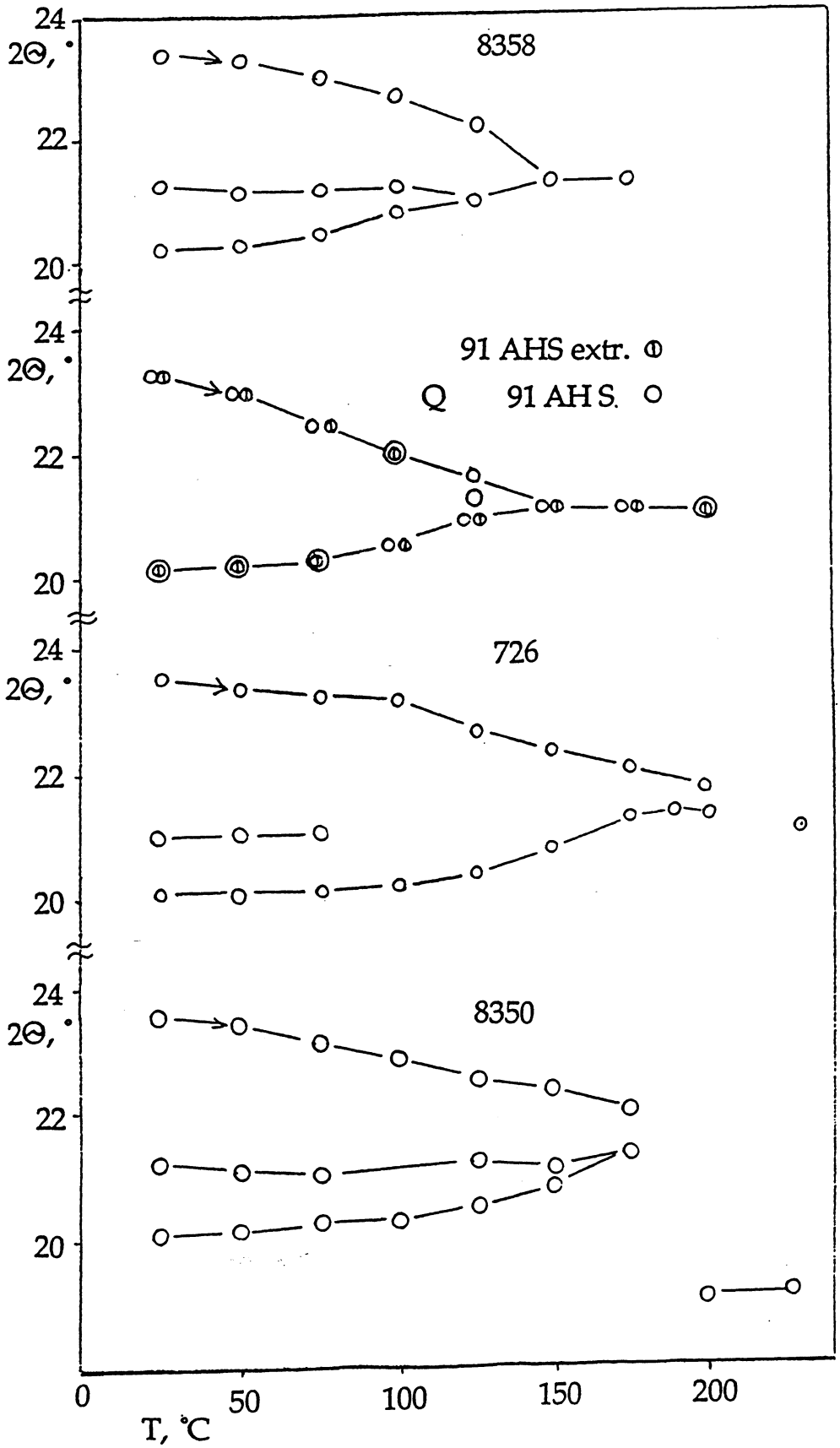

B23. The changes in the 2θ position of the diffraction peaks of samples 8358, 91AHS extracted, 91AHS, 726 and 8350 with increasing temperature from 25°C.

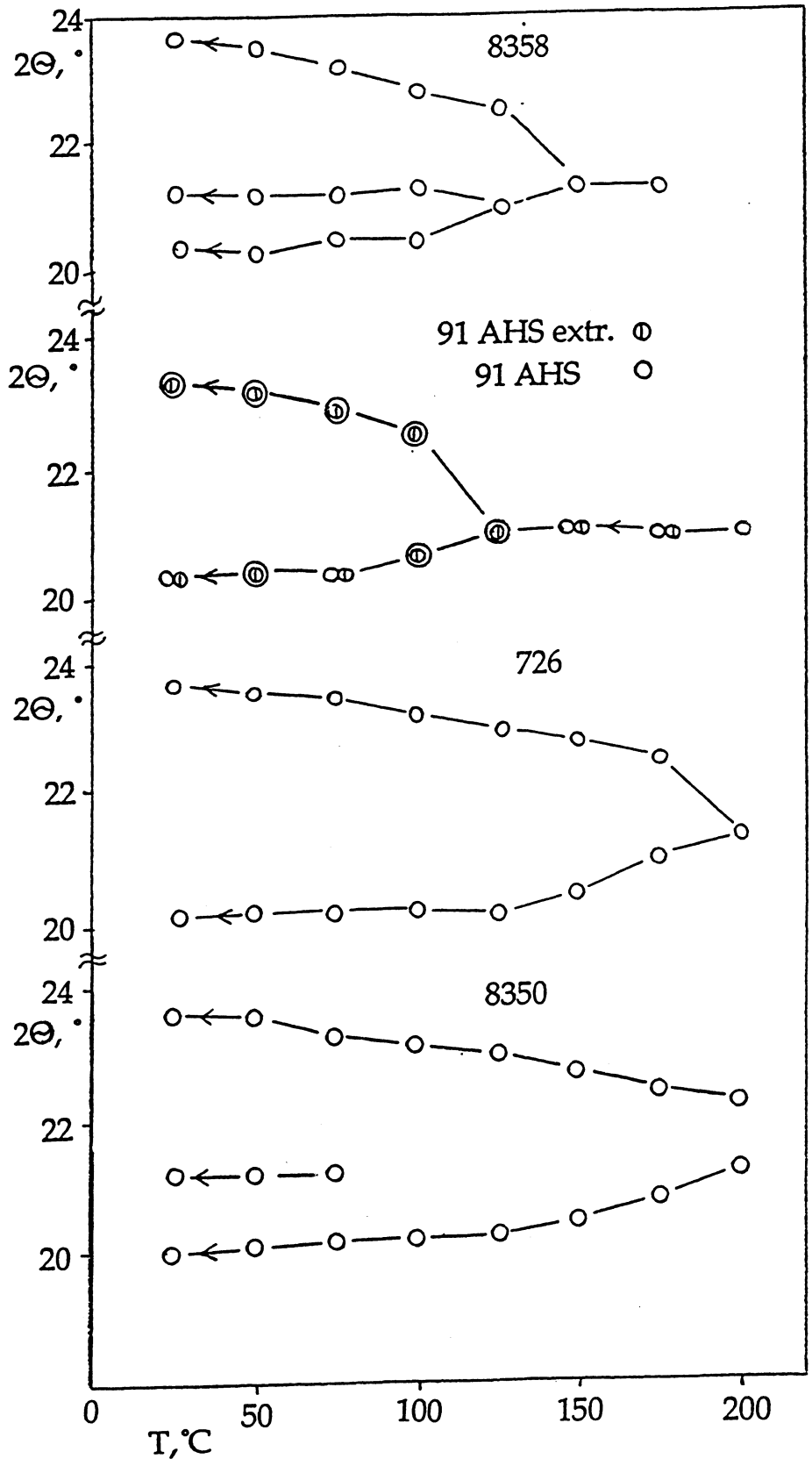

B24. The changes in the 2θ position of the diffraction peaks of samples 8358, 91AHS extracted, 91AHS, 726 and 8350 with decreasing temperature from melt.

C. Characterization of Nylon 6/66 Blends.

As indicated by Parts A and B, nylon 6/66 blends, as well as copolymers and hompolymers, should be appropriate for use as refrigerant barrier films in mobile air conditioning tubing. For 134a, in particular, their permeation qualities are equivalent and physical aging is of no larger concern. The ability to use blends could be more economical than copolymers. This portion of the research was involvedwith their interaction during processing, particularly the effects on crystallization rate (nucleation), mutual solubility (miscibility in the amorphous regions) and crystallization (yielding "defective" crystals). The blend characterization research was conducted on blends prepared from solutions (in formic acid) as well as by melt blending.

The results of this portion of the research have been distributed and published. (Interactions at the PA6/PA66 Interface, F. Rybnikar and P. H. Geil, ACRC TR-04, July 1991 and J. Appl. Polym. Sci., 46, 797 (1992) and Melting and Recrystallization of PA6/PA66 Blends, F. Rybnikar and P. H. Geil, ACRC TR-18, May 1992 and J. Appl. Polym. Sci., 49, 1175 (1993)). They are therefore only summarized here.

The interactions between PA6 and 66 during processing was simulated by placing 2 films of homopolymer of varying relative thickness, as desired for the overall composition, in contact with each other in a DSC pan, heating at 100°C/min to 270°C (10°C above the PA66 T_m), holding the sample at 270°C for 3 min and then cooling to 100°C at 20°C/min while recording the crystallization curve. The sample was then reheated at 20°C/min to 270°C while recording the melting curve. Despite the relatively small area of contact (relative to that in a melt mixed blend of immiscible polymers), considerable mutual interaction was observed (Fig. 1). Especially at low PA6 content, the crystallization range of the PA6 component was broadened and shifted to higher T_c. In addition (not shown

in Fig. 1), an additional T_c peak was observed ca. 10° above the listed T_c of near equal size; this is attributed to nucleation by the already crystallized PA66.

The results suggest a rapid mutual interdiffusion across the laminate interface and at least partial miscibility in the melt (and amorphous regions). There is, at most, only a small degree of co-crystallization, the decreases in T_m indicating defective and/or small crystals. Crystallization rates of the PA6 are enhanced as a result of the presence of already crystallized PA66, i.e. there is a nucleation effect. Using the solution cast blends, which are better mixed, but still segregated at least in the crystalline regions after crystallization, prolonged times in the melt result in a merger and broadening of the PA6 and PA66 crystallization and melting peaks (Fig. 2) suggesting either transamidation (i.e., formation of copolymer) or increasing miscibility. The fact that annealing a sample such as 2' in Fig. 2 at 205°C results in the redevelopment of 2 peaks indicates the effects are due to small, imperfect crystals rather than chemical changes. Overall the results indicate that, although blends could be used for tubing, care needs to be taken in processing to ensure reproducibility, particularly if mixing is poor or melt residence times long.

The second paper indicates the presence of a different, new, more tightly packed crystal structure in the solution cast blends (and homopolymers). The morphology of melt prepared blends is also described, the PA66 component crystallizing first in a loose lamellar framework which serves, at lower temperatures, as nucleation substrates for the PA6. Being found only in the 25°C formic acid cast samples the new crystal structure is not of direct concern relative to tubing materials.

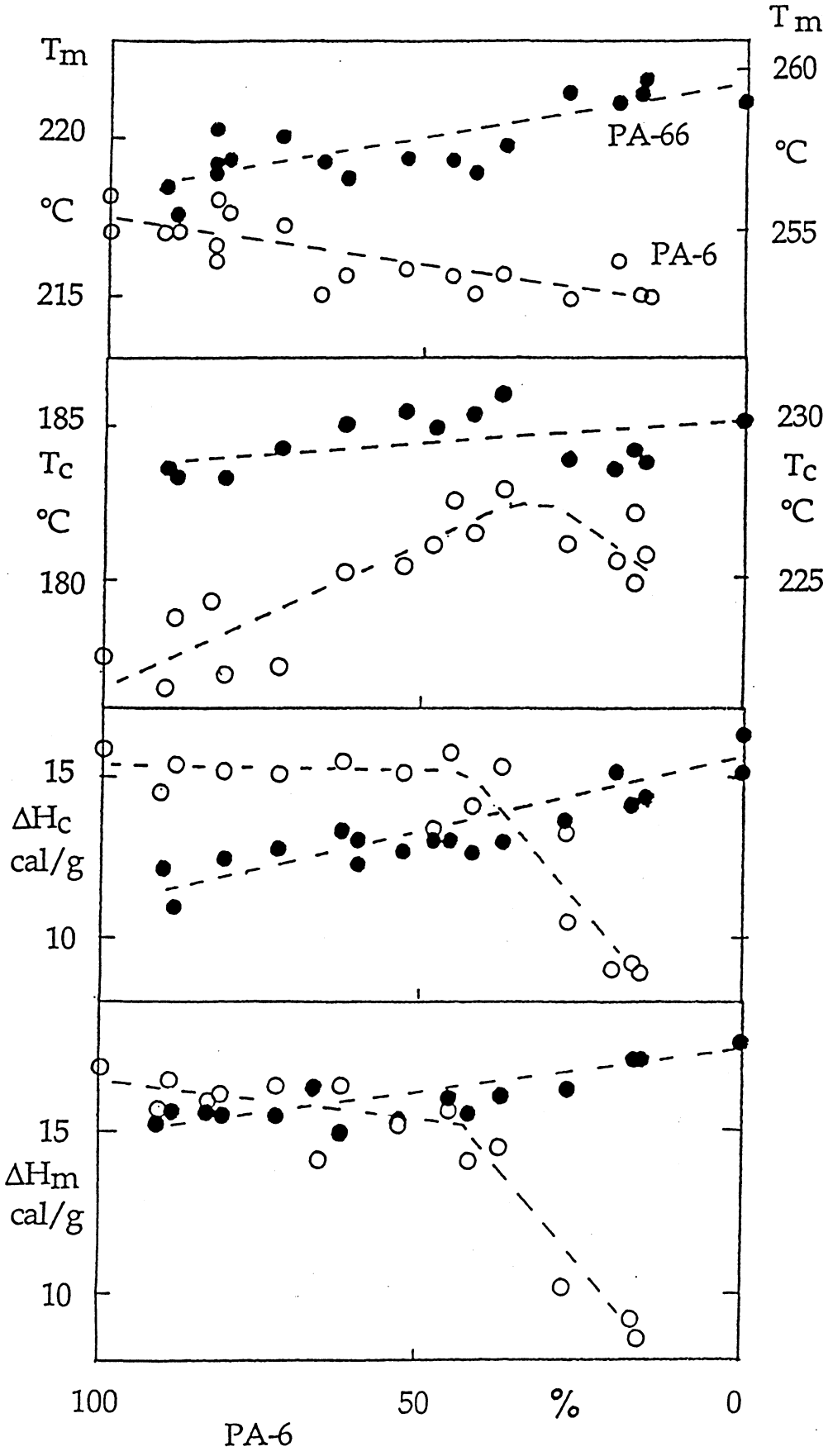

C1. DSC measured melting (second scan) and crystallization (first scan) temperatures and heats of crystallization and fusion of PA6/PA66 contact laminates as a function of composition (i.e. relative film thicknesses).

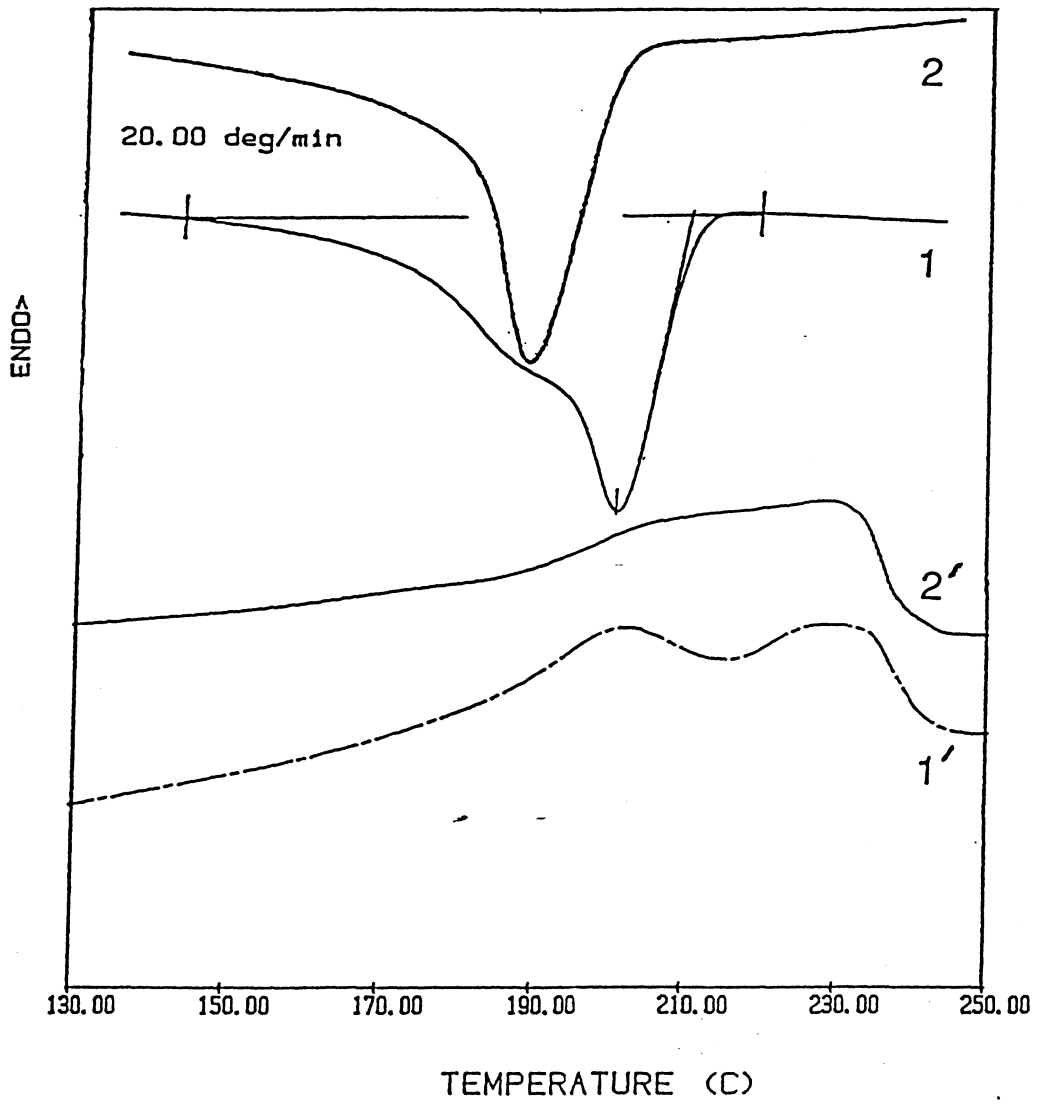

C2. DSC crystallization (1,2) and melting (1', 2') curves for PA6/PA66 1/1 solution blend. Curves 1 and 1' are for a sample previously held at 270°C for 3 minutes, curves 2 and 2' for a sample held at 270°C for 40 minutes.